HIGH-EFFICIENCY, SINGLE-FREQUENCY LASER AND MODULATOR STUDY

R. C. Ohlmann, et al

Lockheed Missiles and Space Company, Incorporated

Prepared for:

Office of Naval Research
Advanced Research Projects Agency

15 June 1974

HIGH-EFFICIENCY, SINGLE-FREQUENCY LASER AND MODULATOR STUDY

Third Annual Technical Report

N-JY-71-24 15 June 1974

R. C. Ohlmann, K. K. Chow, J. J. Younger, W. B. Leonard,
D. G. Peterson, and J. Kannelaud

ARPA Order No. 306
Expiration Date: 15 June 1974
Amount: $399,684

Contract No. N00014-71-C-0049
Program Code 421
Effective Date of Contract: 1 September 1970

Scientific Officer: Director, Physics Programs
Physical Sciences Division
Office of Naval Research, Arlington, Va. 22217

Principal Investigator: R. C. Ohlmann (415) 493-4411, Ext. 45275

Sponsored by

Advanced Research Projects Agency

Lockheed Palo Alto Research Laboratory
LOCKHEED MISSILES & SPACE COMPANY, INC.
A Subsidiary of Lockheed Aircraft Corporation
Palo Alto, California 94304

CONTENTS

Section			Page
	ILLUSTRATIONS		iii
1	INTRODUCTION		1-1
	1.1	Objectives	1-1
	1.2	Laser Communication Systems	1-2
	1.3	List of Publications and Patent	1-2
2	SYSTEM DESIGN		2-1
	2.1	Modulation Formats and Bandwidth Considerations	2-1
	2.2	Quadriphase-Shift-Keying Digital Modulation	2-2
	2.3	FM Analog-Modulation	2-7
3	CRITICAL COMPONENTS AND SYSTEM IMPLEMENTATION		3-1
	3.1	The Optical Modulator	3-1
	3.2	Photodetectors	3-5
	3.3	PN Signal Generator and Biphase Modulators/ Demodulators	3-9
	3.4	The Voltage Controlled Oscillator	3-9
	3.5	The Wideband FM Discriminator	3-9
	3.6	Voltage-Controlled Oscillator/FM Discriminator Tests	3-11
	3.7	System Implementation	3-15
		3.7.1 The 2-Gbit/sec System	3-15
		3.7.2 The 1-GHz FM Analog and 1-Gbit/sec Digital System	3-20
4	SYSTEM TESTS		4-1
	4.1	QPSK Digital Modulation Results	4-1
	4.2	FM Analog and QPSK Digital Modulation Results	4-5
5	LABORATORY DEMONSTRATIONS		5-1
6	CONCLUSIONS AND RECOMMENDATIONS		6-1
7	REFERENCES		7-1

ILLUSTRATIONS

Figure		Page
2-1	Block Diagram Showing Various Subsystems and Modulation Formats Used in the Laboratory Communication System Demonstration	2-3
2-2	2-Gbits/sec Laboratory Laser Communication System: Optical Subsystem and Transmitter Electronics	2-4
2-3	Two Gbit/sec Laboratory Laser Communication System: Receiver Electronics	2-5
2-4	Diagram Illustration: the FM Subsystem and the Combination of FM Analog and QPSK Digital Signals	2-8
2-5	The FM Demodulation System	2-10
3-1	Modulation Index Versus Frequency for 7.5-mm-Length $LiNbO_3$ Crystal With rf Power in Reverse Direction	3-2
3-2	Modulation Index Versus Frequency for 7.5-mm-Length $LiNbO_3$ Crystal With rf Power in Forward Direction.	3-2
3-3	Relative Optical Sideband Power as a Function of Modulation Frequency at Low-Drive Power Levels	3-3
3-4	Modulation Index as a Function of Frequency at 2-W Drive Power Level for the Final Version of the Modulator	3-4
3-5	Relative Frequency Response of the Varian Static Cross-Field Photomultiplier Tube – Test Performed at 0.5145 μm	3-5
3-6	Relative Frequency Response of the TI Silicon Avalanche Diode – Test Performed at 0.5145 μm	3-7
3-7	Relative Frequency Response of the Philco Silicon PIN Diode – Test Performed at 0.5145 μm	3-7
3-8	Relative Response of the Philco Germanium PIN Diode – Test Made at 0.5145 μm	3-8
3-9	Static Voltage Tuning Characteristics of the Final Voltage-Controlled Oscillator	3-10
3-10	Performance Characteristic of the Final Wideband FM Discriminator	3-12
3-11	Experimantal Setup for the VCO/FM Discriminator Tests	3-13

Figure		Page
3-12	Frequency Response of VCO/FM-Discriminator Test Components	3-14
3-13	Output of the FM Discriminator When the VCO Is Swept Between 10 and 470 MHz by the Levelled Sweeper and Driver Amplifier	3-14
3-14	Output of the FM Discriminator When a Compensation Network Is Added to the VCO Driver	3-15
3-15	Transmitter of 2-Gbit/sec Laboratory Optical Communication System	3-16
3-16	Receiver of 2-Gbit/sec Laboratory Optical Communication System	3-19
3-17	FM Transmitter Electronics	3-21
3-18	FM Receiver Electronics	3-22
4-1	Sampling Scope Display of Four 500-Mbit/sec Streams Transmitted Through the Laser Link	4-2
4-2	Waveforms of Two 500-Mbit/sec Streams on 2.5-GHz Subcarrier Frequency With Simultaneous 1-Gbit/sec Digital Signal on 3.5-GHz Subcarrier	4-3
4-3	Waveforms of Two 500-Mbit/sec Streams on 3.5-GHz Subcarrier Frequency With Simultaneous 1-Gbit/sec Digital Signal on 2.5-GHz Subcarrier	4-4
4-4	Complex Microwave Spectrum as Seen at the Output of the Traveling-Wave amplifier	4-8
4-5	Complex Microwave Spectrum As Seen at the Receiver (After Optical Detection and Microwave Amplification)	4-8
4-6	Spectrum of TV Channels 4 and 5 After Transmission Through 1.06-μm Beam, Detection by a Germanium PIN Diode, and Processed to be Ready for Display on TV sets	4-10
4-7	Spectrum of TV Channels 7 and 9 After Transmission Through 1.06-μm Beam, Detection by a Germanium PIN Diode, and Processed to be Ready for Display on TV sets	4-10
4-8	Spectrum of TV Channels 4 and 5 As Received From a High-Gain Antenna and Amplified	4-11
4-9	Spectrum of TV Channels 7 and 9 As Received From a High-Gain Antenna and Amplified	4-11
4-12	Waveforms of the Two 500-Mbit/sec Data as They Appear at Various Stages in the Laboratory Communication System	4-12

Section 1
INTRODUCTION

1.1 OBJECTIVES

The work described in this report is the final year's effort of a three-year program to study wide bandwidth laser communications at 1.06-μm wavelength. Earlier efforts of this program (during the first two years) were directed to studying the means to produce a high-efficiency, single-frequency neodynium doped yttrium aluminum garnet (Nd:YAG) laser operating at 1.06 μm, and to produce high-efficiency, octave-bandwidth, microwave light modulators for this wavelength (Refs. 1 and 2). In addition, a study was also made of laser communication configurations that were suitable for very high data rates. The overall objective of this year's program, then, is to apply the results of these earlier studies to assemble a laboratory communication system that uses the entire modulation bandwidth available. In particular, the final result of this program is to be a laboratory demonstration of a laser-communication system having a bandwidth of 2 GHz.

The detailed objectives of this study program are as follows:

- Design a laboratory communication system, using 1.06-μm radiation from a Nd:YAG laser and having a system bandwidth of 2 to 4 GHz
- Assess the state-of-the-art of high-frequency photodetectors, with emphasis on a cross-field photomultiplier tube (PMT), that offer good frequency and spectral response and are suitable as the receiver elements of this communication demonstration
- Define and design any necessary microwave, digital-modulation, and frequency-modulation subsystems for the communication system
- Assemble and operate the various subsystems
- Demonstrate and evaluate the system performance in a laboratory environment

Work performed during this year has led to the successful achievement of all the objectives listed above.

1.2 LASER COMMUNICATION SYSTEMS

Two laboratory laser communication systems have been designed, implemented, and demonstrated. The first one is a digital communication system employing a quadriphase shift keying (QPSK) modulation format on two microwave subcarriers (2.5 GHz and 3.5 GHz) to carry four data streams totaling 2 Gbit/sec. The second system uses 1 GHz of bandwidth to transmit a number of analog signals by frequency modulating a microwave subcarrier (2.5 GHz), and the second GHz of bandwidth for the QPSK transmission (subcarrier frequency 3.5 GHz) of 1 Gbit/sec digital data. The detected signals at the receiver all show good signal-to-noise ratios. For instance, for the QPSK digital data, it is estimated that by using matched filter detection, the data should be recoverable with only 2- to 3-dB degradation in performance from the theoretical integrate-and-dump performance. For the analog FM transmission, signal-to-noise ratios of 30 dB have been typically measured.

1.3 LIST OF PUBLICATIONS AND PATENT

The following is a list of the publications and patent resulting from the work that has been supported, in total or in part, by this contract during the third year.

1. K. K. Chow, W. B. Leonard, and J. J. Younger, "Recent Advances in Ultrawideband Bandpass Optical Beam Modulators," presented at the 1973 International Electronic Devices Meeting in Washington, D.C., December 1973
2. K. K. Chow, R. C. Ohlmann, R. B. Ward, and R. F. Whitmer, "A 2 Gbit/sec Laboratory Laser Communication System," accepted for publication in the Proceedings of the Sixth DoD Conference on Laser Technology, Colorado Springs, Colorado, March 1974
3. K. K. Chow, "Wide-Band Traveling-Wave Microstrip Meander Line Light Modulator," U.S. Patent 3,791,718, February 12, 1974; assigned to the United States of America as represented by the Secretary of the Navy, Washington, D.C.

Section 2
SYSTEM DESIGN

2.1 MODULATION FORMATS AND BANDWIDTH CONSIDERATIONS

To transmit data at the high rates desired, microwave subcarrier modulation formats are chosen. That is, the information to be transmitted is first modulated onto a microwave carrier frequency (the subcarrier), which, in turn, is modulated onto the optical beam (the optical carrier). For a given modulation format, the data rate to be transmitted determines the required system bandwidth. Therefore, for this demonstration, the data rate has to be chosen so that the entire available microwave bandwidth of the optical modulator is used.

At the present moment, there is no one single data source that will occupy the octave band from 2 to 4 GHz. Therefore, to demonstrate the bandwidth capacity of this laboratory communication system, a convenient way must be devised. This is obtained by transmitting a number of signals filling that band; i.e., the demonstration can be accomplished by using several microwave subcarriers, each with its own sidebands, so as to fill up the entire modulation band of 2 GHz.

To carry out the demonstration in this fashion, two modulation formats have been chosen. One uses quadriphase-shift-keying (QPSK) of a microwave subcarrier to transmit digital signals; the other uses frequency modulation of a microwave subcarrier to transmit analog signals. In this way, both digital- and analog-signal transmission will be demonstrated. In fact, a combination of these two types of signals, filling the 2- to 4-GHz band, can be made to demonstrate simultaneous transmission of digital and analog signals. In the digital QPSK format, two streams of digital data at a rate of 0.5-Gbit/sec each are the most conveniently obtainable signals in a laboratory.*

*For a brief description of QPSK modulation, see subsection 2.2.

Such an arrangement gives a total data rate of 1 Gbit/sec and has sidebands occupying 1 GHz of bandwidth. For FM analog modulation, the modulation bandwidth is typically not limited by the signal sources; rather, it is limited by the devices that impress the modulation onto the subcarrier. One of these devices is usually a voltage-controlled oscillator (VCO) whose instantaneous frequency is a function of the input modulation voltage. For VCO's in this frequency range, a 1-GHz spectrum width is usually around the upper limit of their capabilities.

In this demonstration, therefore, we shall use either (1) two microwave subcarriers, each being QPSK-modulated at 1 Gbit/sec to obtain a total data rate of 2 Gbit/sec; or (2) two subcarriers, one QPSK-modulated to give 1 Gbit/sec and the other modulated by various FM signals to occupy approximately a gigahertz of bandwidth. In this way, both types of modulation signals will be used and performance of the system will be investigated. Figure 2-1 is a block diagram showing the use of these various formats in this demonstration. The choice of subcarrier frequencies for these formats will be discussed in the following subsections.

2.2 QUADRIPHASE-SHIFT-KEYING DIGITAL MODULATION

Detailed block diagrams of this laboratory laser-communication system using QPSK modulation format to transmit a 2-Gbit/sec data stream is shown in Figs. 2-2 and 2-3. The optical subsystem, the digital modulation subsystems, and the modulator driver are shown in Fig. 2-2. The microwave receiver, which amplifies the output of the photodetector, and the subsequent digital demodulation subsystems are shown in Fig. 2-3. The optical subsystem is self-explanatory; the laser and the modulator were both developed under this contract in an earlier phase. The photodetector, however, is a commercial one, and there is yet no one photodetector that is completely satisfactory for our demonstration. This point will be elaborated in subsection 3.2.

In such a digital QPSK modulation subsystem, a cw microwave signal is used as a subcarrier. Modulation of the subcarrier by the digital data results in a change of the rf phase of the subcarrier. These are shown in detail in the phasor diagram presented in

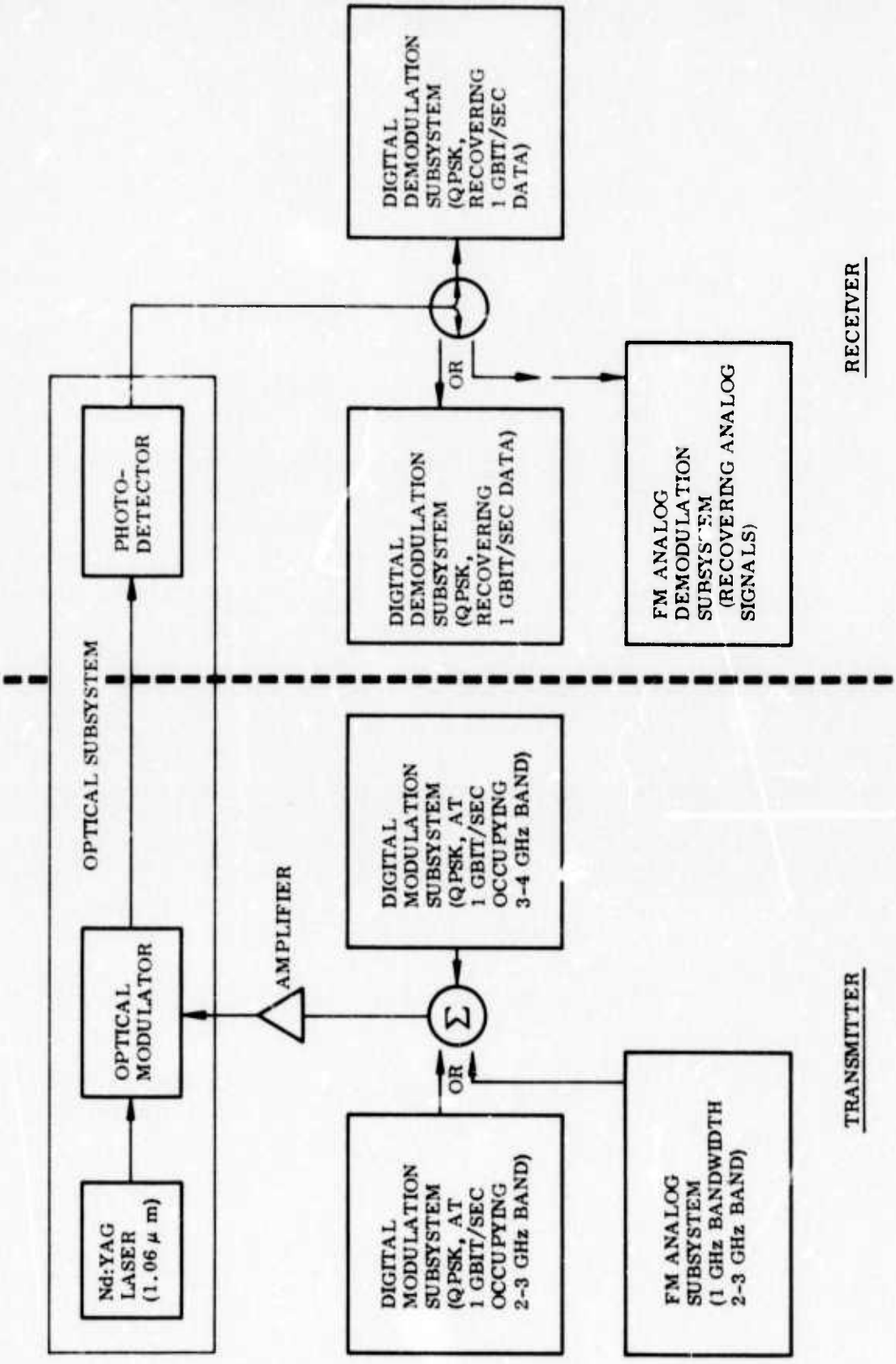

Fig. 2-1 Block Diagram Showing Various Subsystems and Modulation Formats Used in the Laboratory Communication System Demonstration

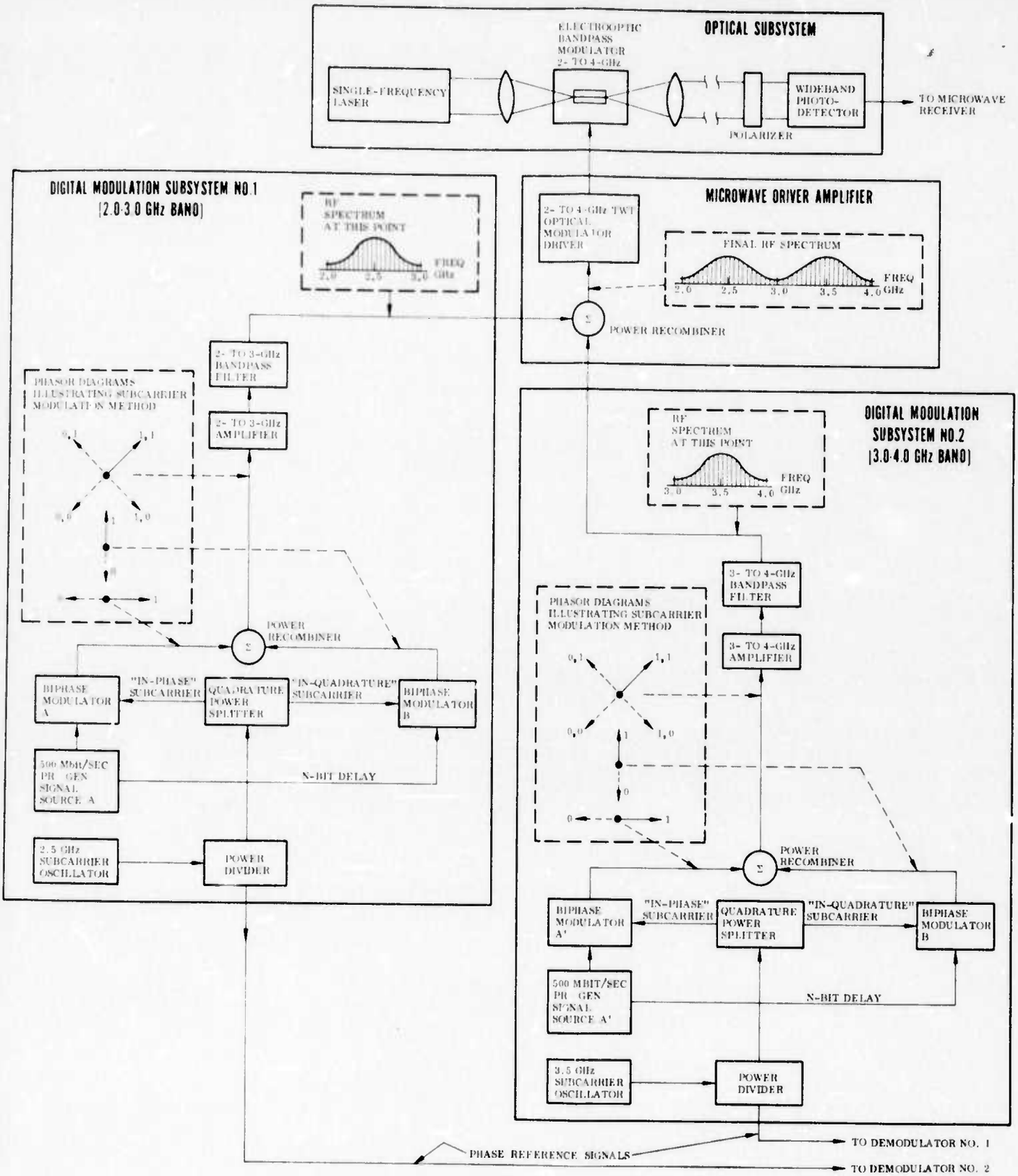

Fig. 2-2 2-Gbit/sec Laboratory Laser Communication System: Optical Subsystem and Transmitter Electronics

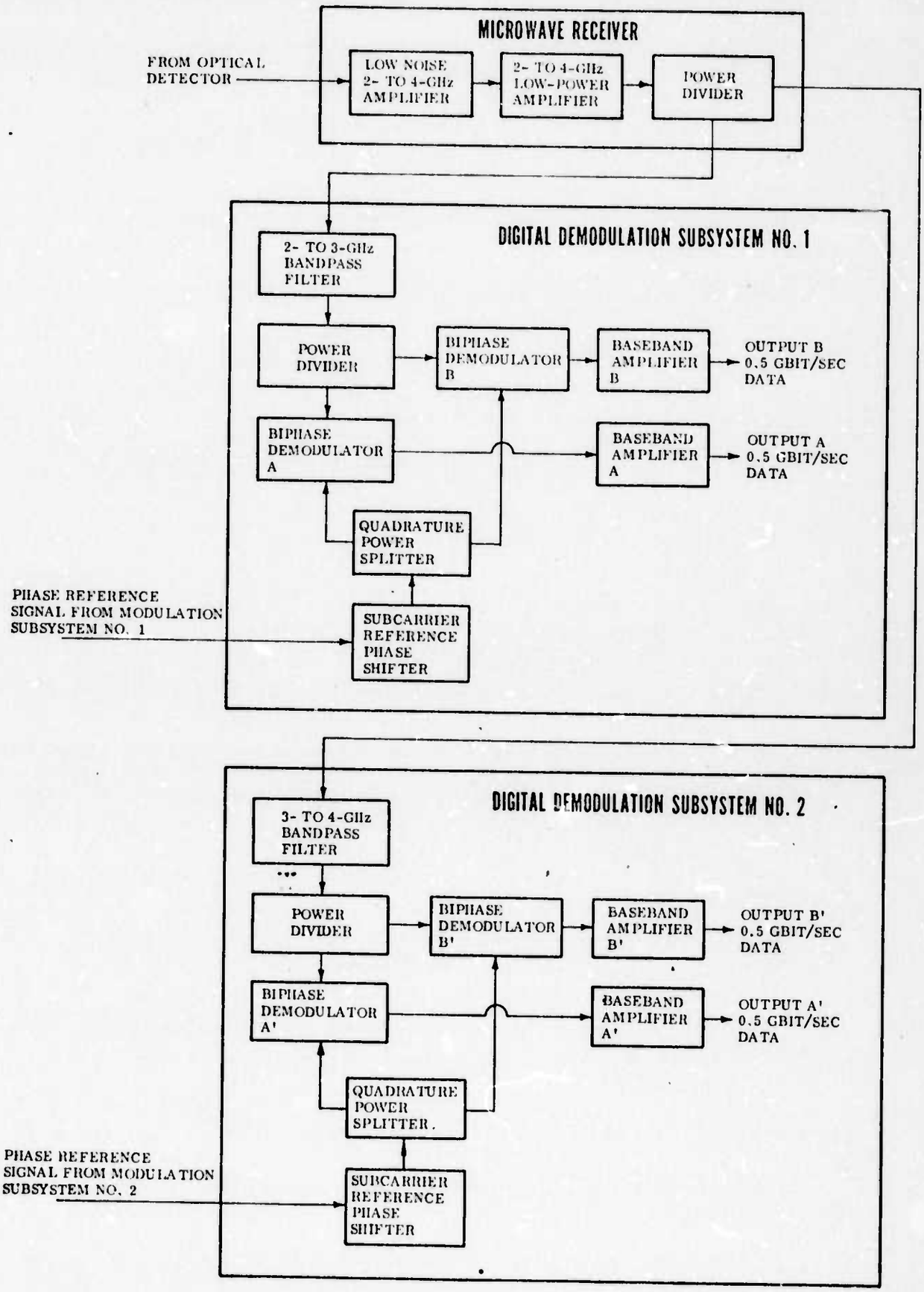

Fig. 2-3 Two-Gbit/sec Laboratory Laser Communication System: Receiver Electronics

Fig. 2-2. Because of the required bandwidth considerations, as discussed in subsection 2.1, two subcarriers are chosen – one at 2.5 GHz, and the other at 3.5 GHz. Each subcarrier is split into two channels: one "in-phase" channel and one "in-quadrature" channel. Each of the channels is then biphased-shifted at a biphase modulator by an independent 500-Mbit/sec simulated data stream from a pseudo-random (PR) signal generator as shown in the associated phasor diagram in Fig. 2-2. That is, the phase of the microwave subcarrier of that channel is reversed at each change of state of the signal at the binary input terminal of the biphase modulator. Thus, if the modulating signal is a binary "1," the phase of that channel is undisturbed. If, on the other hand, the modulator signal is a binary "0," the phase of that channel is reversed (switched by 180 electrical degrees as shown dotted in the phasor diagram).

Since the two channels are already in quadrature, the two biphase modulators will give four possible quadrature phase relationships. Therefore, the combination of the two channels results in the final phasor relationship shown in Fig. 2-2 and gives a total data rate of 1 Gbit/sec for that subband.

At an input data rate of 1 Gbit/sec, the sideband power of QPSK modulation has first nulls at 500 MHz above and below the subcarrier frequency. Outside the first nulls, the power content is negligible. Therefore, for each subband, the center frequency of the subband is chosen as the subcarrier frequency (2.5 and 3.5 GHz as mentioned earlier), and a 1-GHz bandpass filter (2 to 3 GHz and 3 to 4 GHz) is used to reject the sideband power outside the first nulls. Combination of these two subbands gives a total data rate of 2 Gbit/sec. This is amplified by a 10-W traveling-wave tube (TWT) to drive the optieal modulator.

In the photo[illegible]ector, the optical carrier is detected to recover the microwave subcarriers and their sidebands which are then sent to the first amplifier in the receiver subsystem. After amplification, the microwave signal is divided into two halves as shown in Fig. 2-3. Each half is filtered to give one of the subbands which is then further divided into two channels. The signal in each channel, together with a strong

"in-phase" or "in-quadrature" reference, is directed to a biphase demodulator. In a communication system, the reference signals required are normally derived from the incoming signals. For the ease of this demonstration, however, the reference signals are taken from the transmitter directly by separate cables (hardwire references) to demonstrate the capacity of the laser communications system, without having to deal with the added complications of phased-locked loops, etc. for the derivation of the reference signals. These hardwire references are clearly indicated in Figs. 2-2 and 2-3.

The biphase demodulator performs synchronous demodulation of the received QPSK signal by comparing its phase with that of the reference signal. The output signal of the biphase modulator is filtered and amplified by a baseband amplifier to recover the 500 Mbit/sec digital data at each channel. This will be discussed in greater detail in subsection 3.3. Two 500-Mbit/sec streams are recovered for each subband, i.e., a total of 2 Gbit/sec data is recovered from both subbands.

It should be emphasized here that, although the 500-Mbit/sec PR signals for both channels in the subband are synchronous as used here in the demonstration, this system will accept asynchronous data with only minor degradation. This has been demonstrated in an earlier experiment conducted at LMSC (Ref. 3).

2.3 FM ANALOG-MODULATION

For the transmission of analog signals, frequency modulation of a microwave subcarrier is chosen. The block diagram for this particular form of modulation is shown in Fig. 2-4; the heart of the modulation subsystem is the voltage controlled oscillator (VCO). The VCO accepts amplified baseband analog signals (e.g., from local TV stations) and uses them to control a voltage-sensitive tuning element of the oscillator, typically a varactor diode. Thus, the instantaneous output frequency of the oscillator is proportional to the instantaneous voltage of the analog signal. For this experiment, several local TV channels, as well as an audio signal source which modulates a narrow band FM (NBFM) 400-MHz signal generator, are chosen so that the sidebands

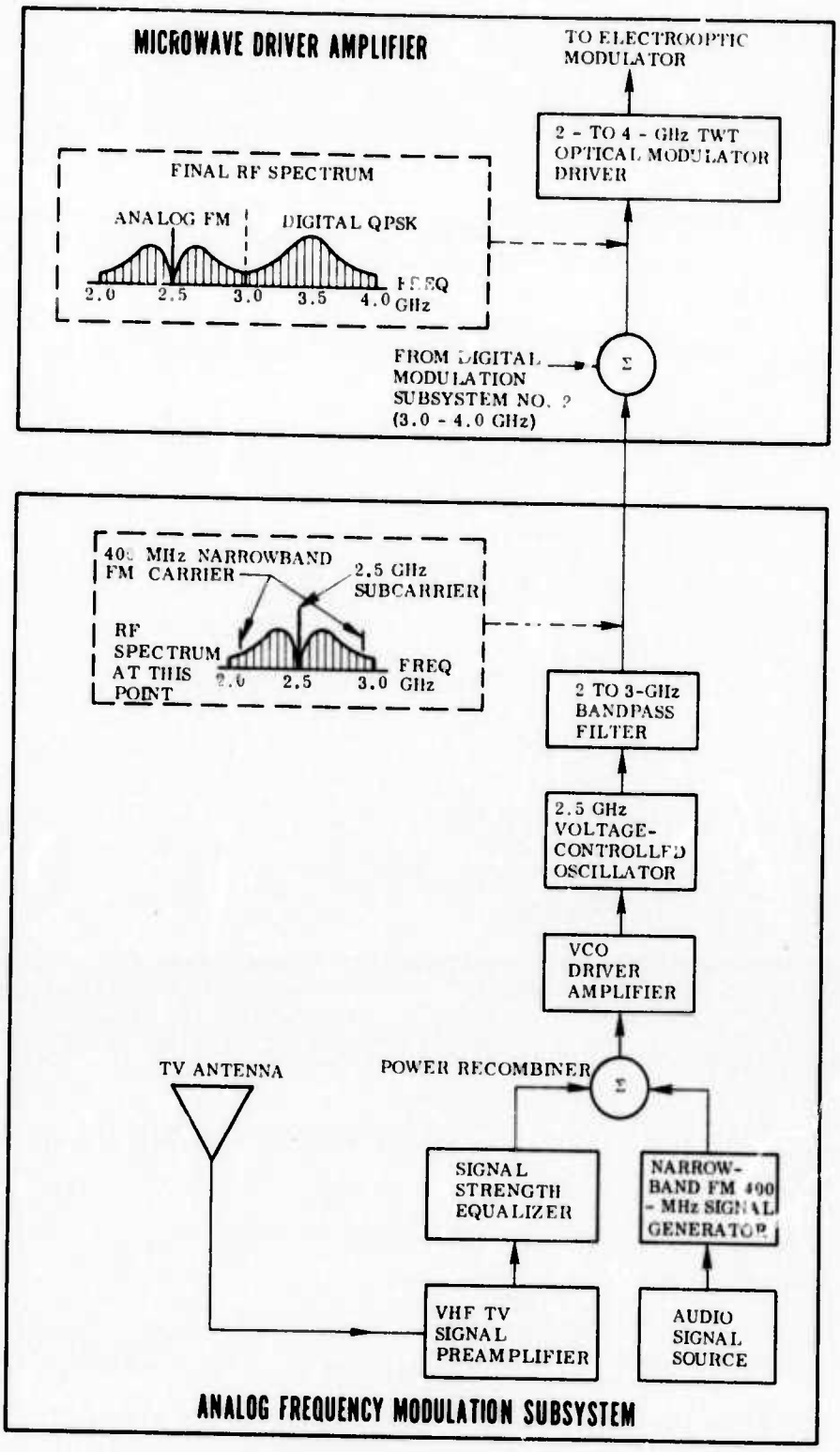

Fig. 2-4 Diagram Illustration: the FM Subsystem and the Combination of FM Analog and QPSK Digital Signals

of the VCO occupy practically the entire gigahertz band. TV signals and audio FM 400-MHz signals are combined, amplified, and used to control the frequency of the VCO. At the beginning of this experiment, the microwave subcarrier for the FM subband was chosen to be 3.5 GHz because it was believed that VCOs having 400 MHz of linear tuning range could be obtained more easily at a 3.5-GHz center-frequency. However, experience gained during this program showed that such was not necessarily the case. In addition, the poor frequency response of photodetectors at the high-frequency end (2- to 4-GHz band), coupled with the requirement that analog TV signals require rather high signal-to-noise (S/N) ratio to attain good reception and presentable pictures, changed our earlier thoughts about the choice of this subcarrier frequency. As a result, 2.5 GHz is now used as the subcarrier frequency for the analog signals, and system demonstrations performed using this subcarrier frequency have given satisfactory results.

In this experiment, the TV signals and the 400-MHz NBFM signal are combined and amplified to drive the VCO. From the VCO, the signal is passed through a 2- to 3-GHz bandpass filter to eliminate undesirable sidebands and spurious signals. The rf spectrum at that point (after the bandpass filter) is then as shown in Fig. 2-4. This signal is sent to the power recombiner to replace the lower subband of the digital QPSK signals (the 2- to 3-GHz subband) as shown in Fig. 2-1. After combination with the upper subband containing the other digital QPSK signals (the 3- to 4-GHz subband), the combined signal is sent to the traveling wave tube (as shown in Fig. 2-2) for the modulation of the optical signal.

The demodulation system for the FM subband is rather simple as shown in Fig. 2-5. The received signal from the photodetector is again split into two halves; one of them goes to the 3.5-GHz subcarrier digital demodulation circuit as before, while the other is directed to the FM demodulation subsystem as shown in Fig. 2-5. This signal is filtered by a 2- to 3-GHz bandpass filter and sent through a wideband FM discriminator. It is then amplified by a baseband amplifier to recover the TV signals and the 400-MHz NBFM signal.

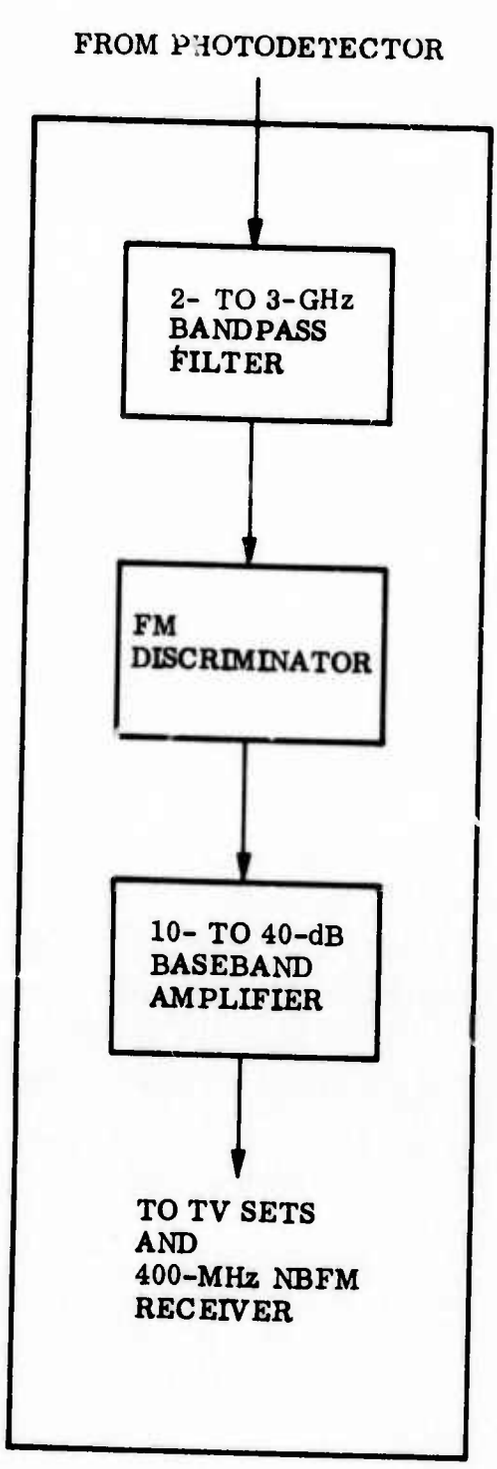

Fig. 2-5 The FM Demodulation System

Section 3
CRITICAL COMPONENTS AND SYSTEM IMPLEMENTATION

Most of the critical components required for the system demonstration have been discussed in some detail in the Third Semiannual Report (Ref. 4). Therefore, their performance will be presented here only briefly. For additional information, reference is made to the Third Semiannual Report. However, the changes that have been made during the last six months will be discussed in some detail here.

3.1 THE OPTICAL MODULATOR

During the first six months, additional effort was spent in improving the 2- to 4-GHz electrooptic modulator, since this modulator is the heart of this demonstration. In particular, the "reverse-flow" mode of operation was carefully investigated. This is the mode in which the rf drive power for the optical modulator flows through the circuit in such a way that the electrooptic modulating crystal is at the input digit. Through painstaking tuning and matching procedures, improved performance over the "forward-flow" mode was obtained, as shown in Fig. 3-1. At a 6-W input drive level, an average of 60-percent modulation index across a 3-dB bandwidth of 2.07 to 4.00 GHz is obtained. This is a definite improvement over the "forward-flow" mode obtained last year, shown in Fig. 3-2 as a comparison, for which approximately 62-percent average modulation index was obtained at about a 10-W drive level.

It appears from Fig. 3-1 that the modulator was tuned to a higher passband than the desired 2 to 4 GHz, because the low-frequency end showed a sharp drop while the high-frequency end showed uniform response to the band-edge. Therefore, additional turning effort was applied to move the passband lower. This was met with some success: Fig. 3-3 shows the relative optical sideband power as a function of modulation frequency at low-drive power levels. At these drive levels and using this particular

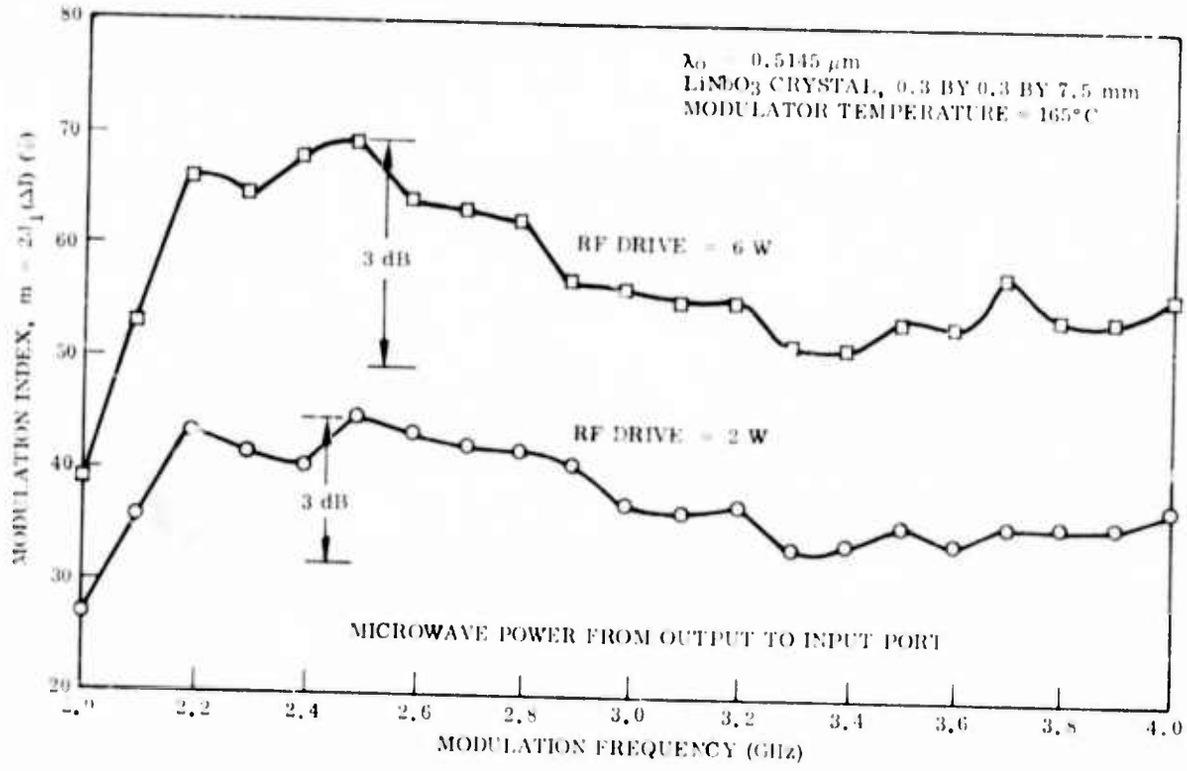

Fig. 3-1 Modulation Index Versus Frequency for 7.5-mm-Length $LiNbO_3$ Crystal With rf Power in Reverse Direction

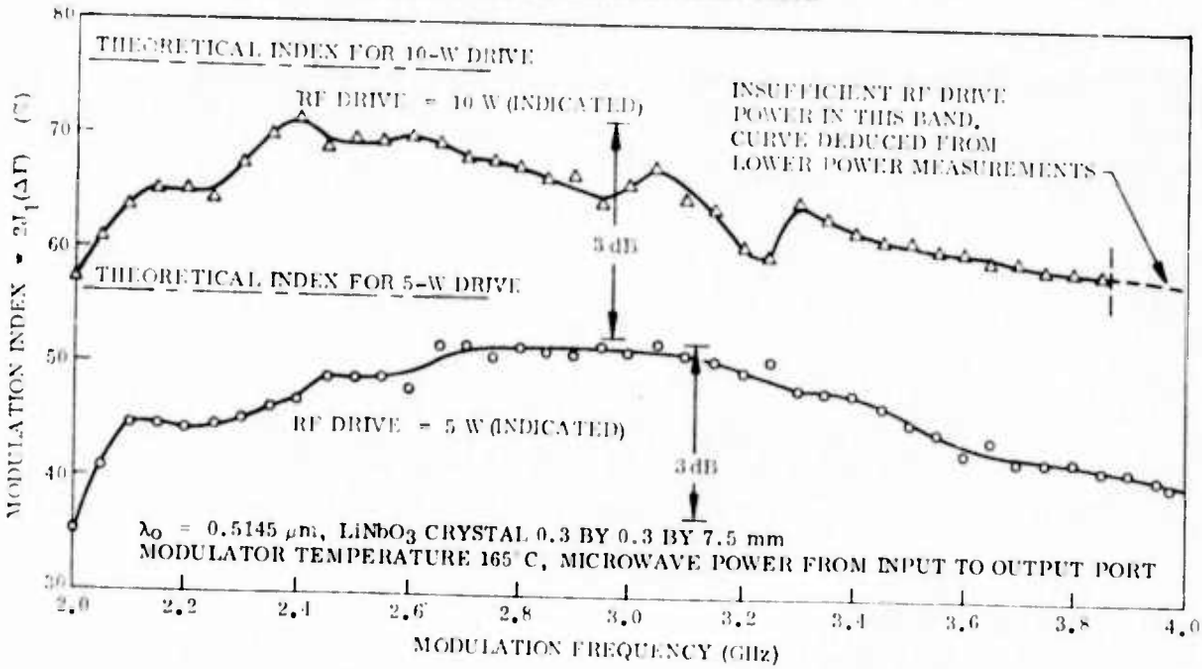

Fig. 3-2 Modulation Index Versus Frequency for 7.5-mm-Length $LiNbO_3$ Crystal With rf Power in Forward Direction. (Results were obtained last year and are included here for purpose of comparison)

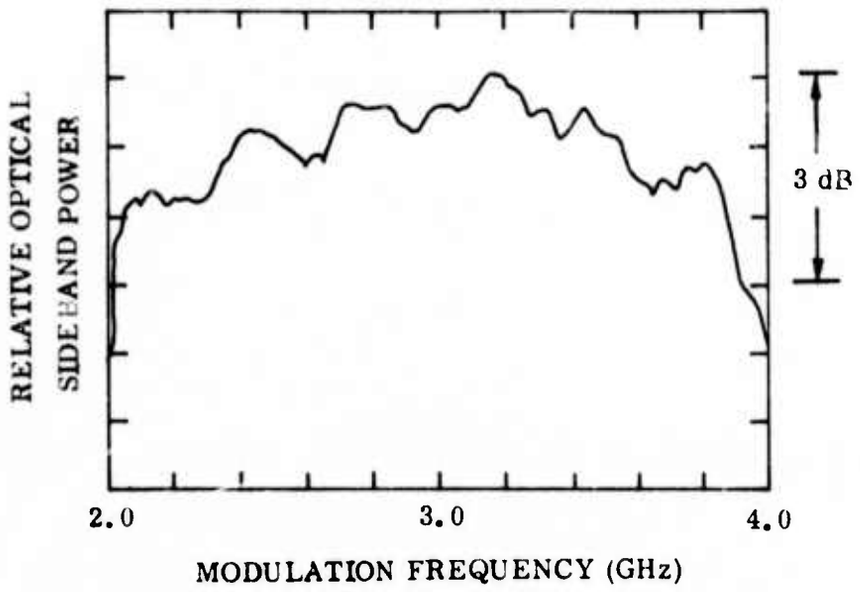

Fig. 3-3 Relative Optical Sideband Power as a Function of Modulation Frequency at Low-Drive Power Levels

method of measurement, the modulation index m is approximately proportional to the square of the sideband power. Thus, the 3-dB level is about half-way down from the peak, as indicated in Fig. 3-3, and no increase in bandwidth over that shown in Fig. 3-1 is observed. Actual measurement of modulation index near the peak response showed that 80-percent modulation index for 0.5145 μm was obtainable at 8.3 W of rf drive power; this value also agrees well with that scaled up from Fig. 3-1. However, the peak response is now considerably broader and more centered in the passband than that shown in Fig. 3-1. In this respect, improvement in modular performance has been achieved.

This modulator was used in the initial tests for the 2-Gbit/sec data transmission and performed well, as reported in the Semiannual Report (Ref. 4). Unfortunately, in the initial experiments for the 1-GHz analog and the 1 Gbit/sec digital transmission, the

electrooptical crystal inside the modulator was fractured. A new modulator crystal was substituted into the modulator. Because of the schedule, it was not possible to make detailed tuning and matching to duplicate the results obtained earlier. Modulation index as a function of frequency, obtained for the final version of the modulator, is as shown in Fig. 3-4. Obviously, the performance was not as good as that obtained earlier, but this proved adequate for the demonstration of the 1-GHz analog and the 1-Gbit/sec digital data transmission. Laboratory measurements indicate that approximately 35-percent modulation index is repeatedly obtainable at 2.0 W of rf drive at 3 GHz.

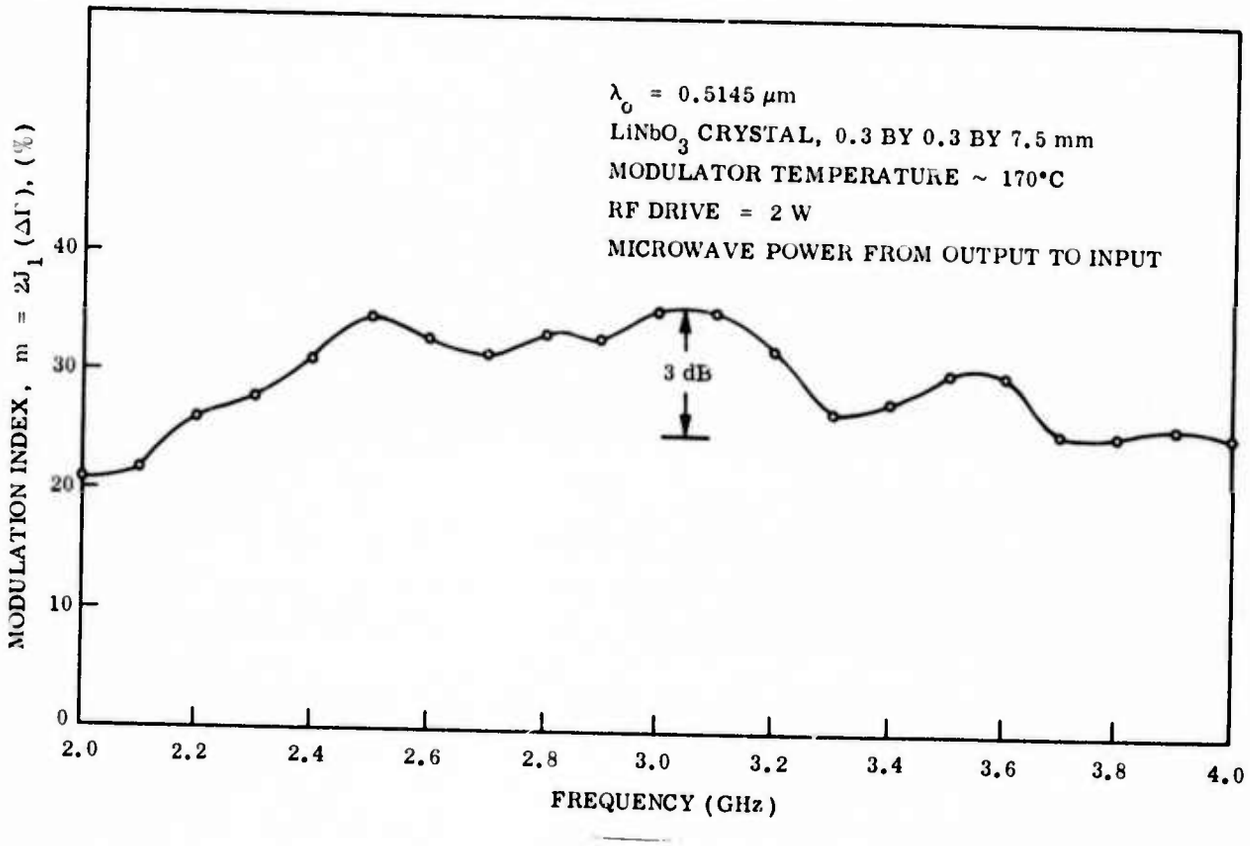

Fig. 3-4 Modulation Index as a Function of Frequency at 2-W Drive Power Level for the Final Version of the Modulator

3.2 PHOTODETECTORS

For the laboratory demonstration, an experimental static cross-field photomultiplier tube (CFPMT) having a III-V compound (InGaAsP) photocathode was ordered from Varian Associates. This order was initiated in the belief that good quantum efficiency, low-noise figure, and good frequency response at 4 GHz could all be obtained under a "best-effort" arrangement. Unfortunately, the CFPMT received falls short of our expectations: quantum efficiency is less than 1 percent, frequency response above 3.5 GHz is poor and, worst of all, there is a spurious resonance at about 2.5 GHz, which is also one of the subcarrier frequencies. The frequency response of the CFPMT is shown in Fig. 3-5. (The method used to determine the frequency response will be discussed in the following paragraphs.) Therefore, this CFPMT was deemed undesirable for our experiment. Another CFPMT, which did not have good quantum efficiency but did not appear to have this strong resonance, was used for the detection of 2-Gbit/sec optical data transmission.

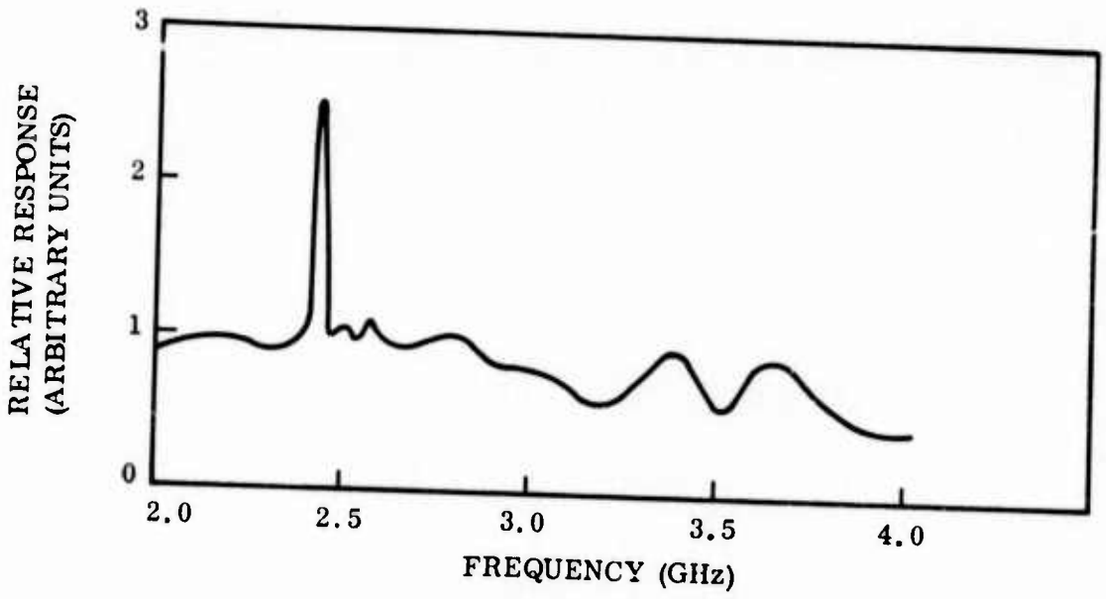

Fig. 3-5 Relative Frequency Response of the Varian Static Cross-Field Photomultiplier Tube – Test Performed at 0.5145 μm

Since the CFPMT specially ordered from Varian Associates did not fulfill our requirements, much effort was expended in the selection of a suitable photodetector. Solid-state photodiodes were investigated; these included silicon PIN diodes, germanium PIN diodes, as well as a silicon avalanche diode. All these diodes have rather low frequency response in the 3- to 4-GHz range; however, both silicon and germanium PIN diodes appeared useful. Test results are briefly described below.

In these tests, the frequency response of the optical modulator was first determined by measuring the optical sideband power as a function of modulation frequency in a Fabry-Perot scanning interferometer. The modulated laser beam is then detected by the photodetector under test. The output of the photodetector is fed into a microwave spectrum analyzer, swept at a very low frequency. The frequency response as displayed on the cathode-ray tube of the spectrum analyzer then gives the combined effects due to the optical modulator and the photodetector. That is, the display gives the apparent received microwave power as a function of frequency. Since the received power is proportional to the square of the modulation index, the apparent modulation index as seen by the spectrum analyzer can be obtained by taking the square root of the power spectrum. When this apparent modulation index is divided by the known modulation index for the optical modulator as measured previously, frequency response of the photodetector is obtained. For convenience, these tests were initially made at 0.5145 μm. Those having favorable frequency response were later tested at 1.06 μm.

Figure 3-6 is the frequency response curve for a commercial silicon avalanche diode (TI Model XL 55). It is seen that beyond 3.0 GHz, the response was very poor. Since the avalanche noise was also very high, the diode was not useful even at the visible wavelength. There is a germanium avalanche diode (TI XL 57) available for 1.06-μm wavelength. Specifications on its frequency response and noise characteristic are much worse than those of TI XL 55. Therefore, the germanium avalanche diode was not seriously considered.

Figure 3-7 is the response curve for a silicon PIN diode (Philco Model 4501). This diode has a rather small junction capacitance (0.8 pF typical), so that its frequency

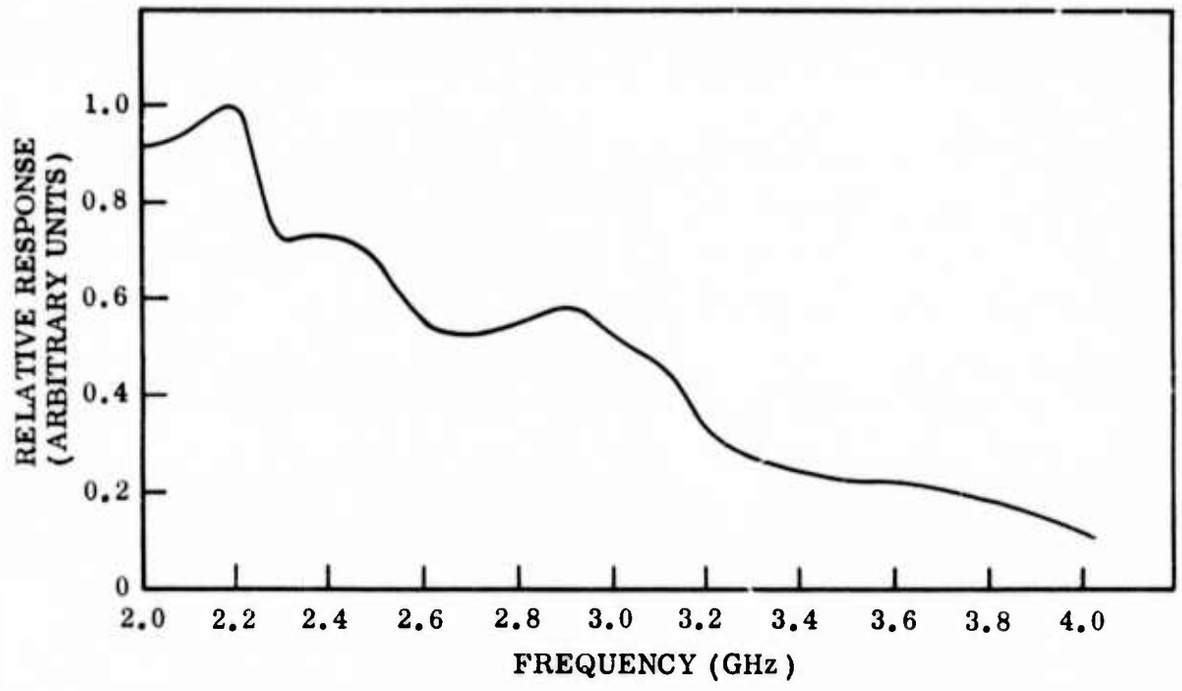

Fig. 3-6 Relative Frequency Response of the TI Silicon Avalanche Diode – Test Performed at 0.5145 μm

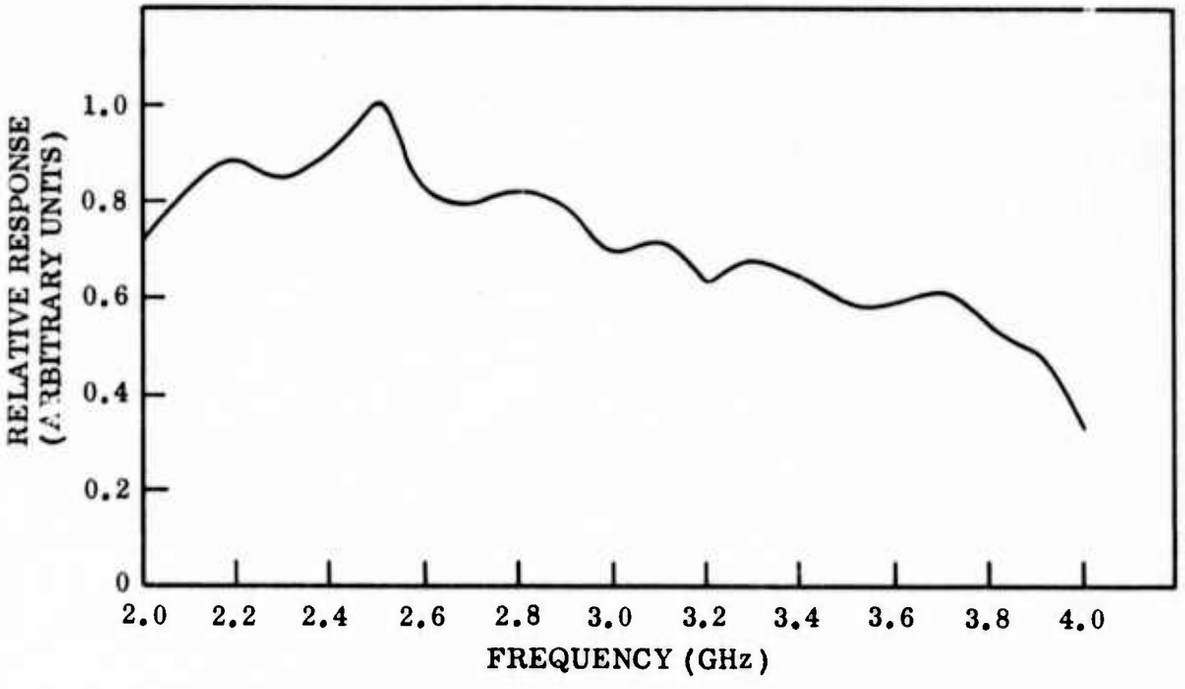

Fig. 3-7 Relative Frequency Response of the Philco Silicon PIN Diode – Test Performed at 0.5145 μm

response is reasonably good even in the 3- to 4-GHz range. Unfortunately, the spectral response at 1.6 μm was very poor, thereby rendering the diode not very useful for this demonstration. For laboratory use with visible wavelengths, however, this diode is probably the most desirable one.

Figure 3-8 shows the frequency response of the Philco Germanium PIN diode (Model 4529). This diode has a large junction capacitance (~ 5 pF), and consequently worse frequency response, than the silicon PIN diode tested above. Beyond 2.6 GHz, there is not much response. However, since the diode is spectrally sensitive at 1.06 μm and can withstand much light intensity, it is still the best detector for the 1.06-μm experiments. It is therefore chosen for the 1.06-μm tests.

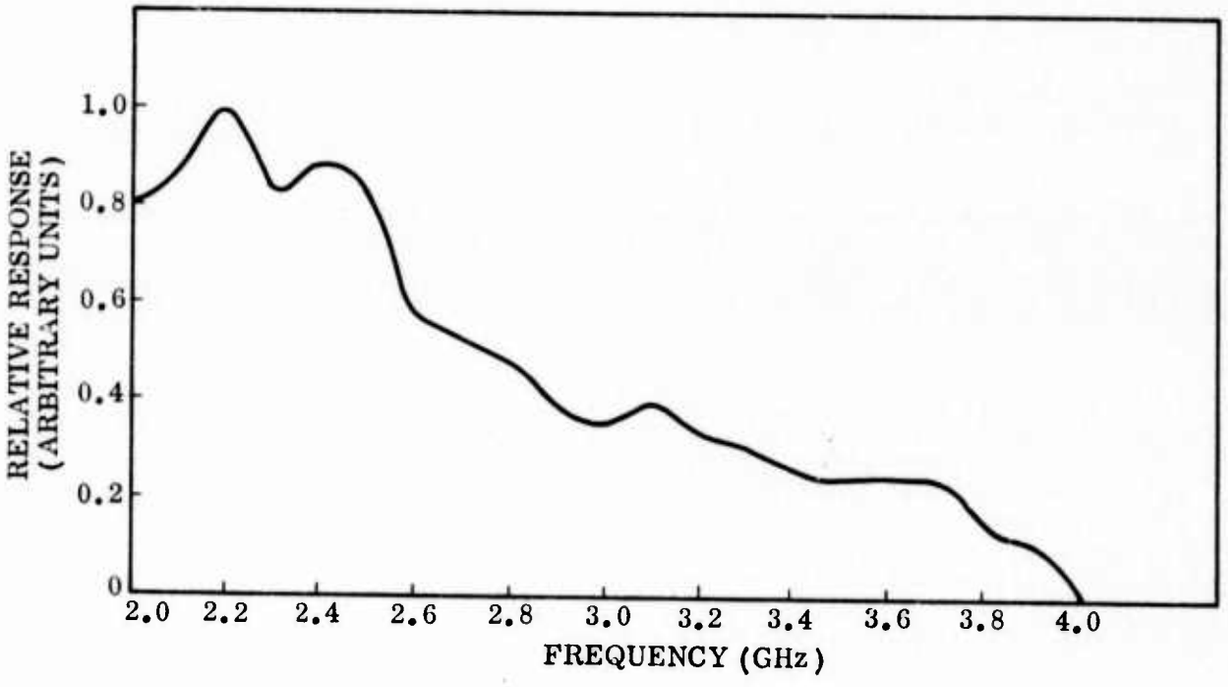

Fig. 3-8 Relative Response of the Philco Germanium PIN Diode – Test Made at 0.5145 μm

3.3 PN SIGNAL GENERATOR AND BIPHASE MODULATORS/DEMODULATORS

In the digital modulation subsystem, two important subassemblies are required. These are the 500-Mbit/sec pseudorandom (PR) signal generators and the balanced biphase modulators. Both devices have been discussed extensively in the Third Semiannual Report (Ref. 4) and will not be repeated here.

3.4 THE VOLTAGE CONTROLLED OSCILLATOR

Originally, the subband used for the transmission of 1-GHz bandwidth analog signals was the 3- to 4-GHz band. The performance of two VCO's operating in this band has been reported in the Third Semiannual Report (Ref. 4). Because of the poor frequency response of the photodetectors as well as the nonlinearity problems in the VCO drivers, it was decided to use the 2- to 3-GHz subband for the transmission of analog signals (see Ref. 4). For this reason, a new VCO was ordered from Omni-Spectra having a center frequency of 2.5 GHz. This VCO was received at the end of the third quarter and showed excellent performance characteristics as shown in Fig. 3-9. The overall linearity over the tuning range of 2.23 to 2.275 GHz was good. In particular, over a tuning range of 160 MHz (± 80 MHz) centered at 2.5 GHz, excellent linearity is obtained. The voltage required for this ± 80 MHz deviation is only 1.5 V peak-to-peak, corresponding to an rms drive power of 6 mW. Thus, this VCO showed much better response than any of the previous ones and is most appropriate for the FM subsystem.

3.5 THE WIDEBAND FM DISCRIMINATOR

For the demodulation of analog signals, a wideband FM discriminator is required. The desired characteristics of the FM discriminator are as follows:

- Good linearity over a frequency range of 2- to 3-GHz and ability to handle modulation frequencies up to 400 MHz
- High sensitivity to input frequency variation and low sensitivity to input amplitude variations

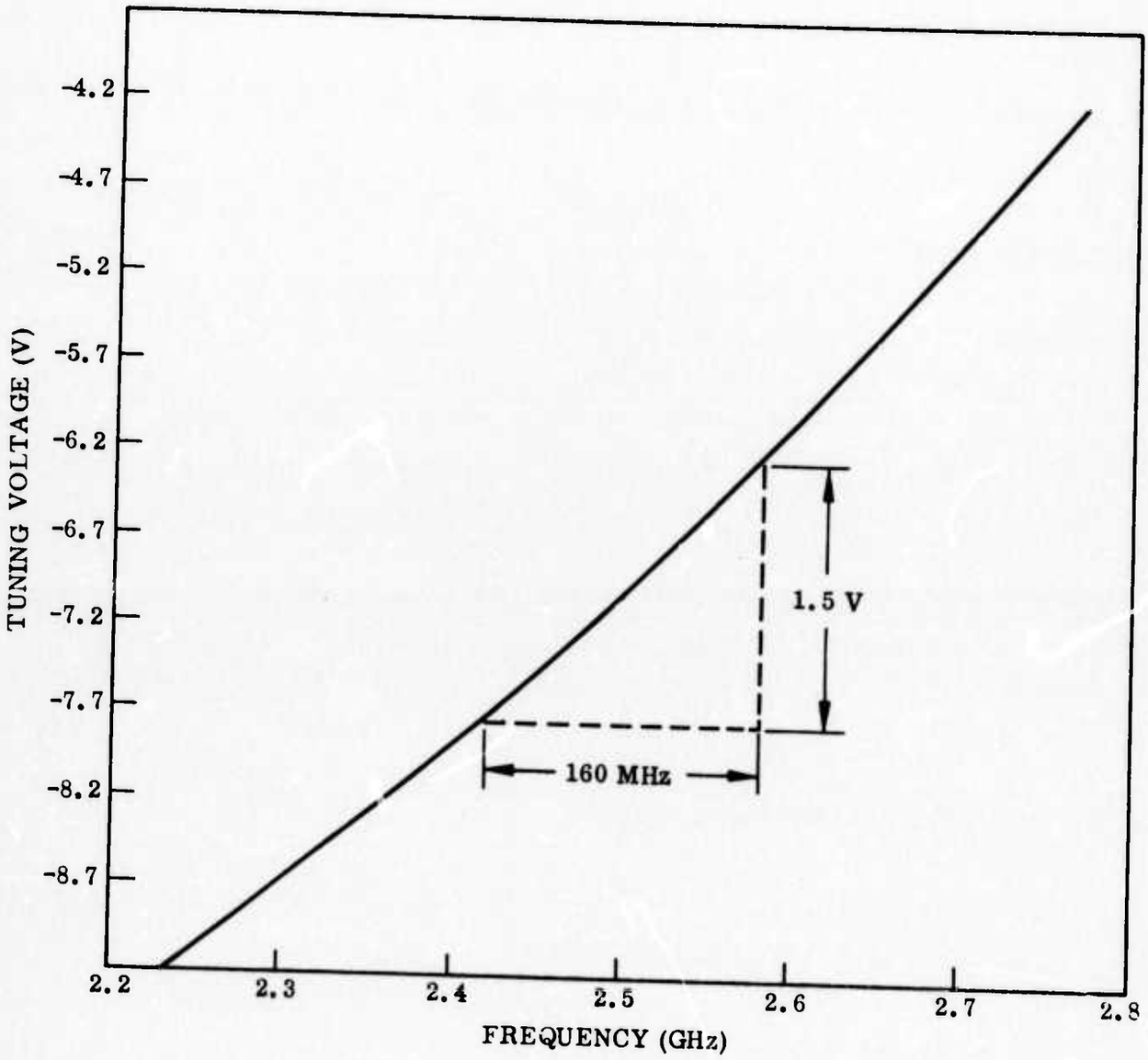

Fig. 3-9 Static Voltage Tuning Characteristics of the Final Voltage-Controlled Oscillator

- Output level high enough that the noise in the succeeding 400-MHz wide-baseband amplifier does not appreciably degrade the signal-to-noise ratio established in the photodetector

The design of wideband discriminators has been accomplished at LMSC; it is based on the work of Kincheloe and Wilkens (Refs. 5 and 6), who suggested the use of a microwave power divider and a 3-dB hybrid coupler connected by constant impedance transmission lines. The arrangement is a microwave analog of a one-dimensional optical interferometer; its theory of operation has been presented in the Third Semiannual Technical Report (Ref. 4).

During the first half year, a discriminator operating in the 3- to 4-GHz subband has been fabricated and tested. Linearity was good for deviations up to 250 MHz, as reported in the Third Semiannual Technical Report (Ref. 4). Because of the change of the frequency modulation subband, a new FM discriminator had to be fabricated. This was done in the third quarter and the results are as shown in Fig. 3-10. Over a deviation of ± 80 MHz, the output of the discriminator is linear. Linearity over a greater range can be obtained by carefully changing the lengths of the two interfering paths. Since this linearity range is more than adequate for the VCO, no additional work was performed.

3.6 VOLTAGE-CONTROLLED OSCILLATOR/FM DISCRIMINATOR TESTS

To determine whether the voltage-controlled oscillator (VCO) and the FM Discriminator will perform properly in the system tests, both were connected together and their combined performance was evaluated. The test setup is as shown in Fig. 3-11. The VCO is driven by a baseband amplifier having a flat response up to 550 MHz. The output of the VCO is filtered by a bandpass filter and fed into the FM discriminator. The output of the discriminator is filtered by a low-pass filter having its cutoff at 470 MHz. The lowpass filtered output is fed to a spectrum analyzer and the resulting power spectrum displayed on the cathode ray tube. Figure 3-12 shows the frequency response characteristic of the baseband amplifier. The lower trace is a levelled output of the swept

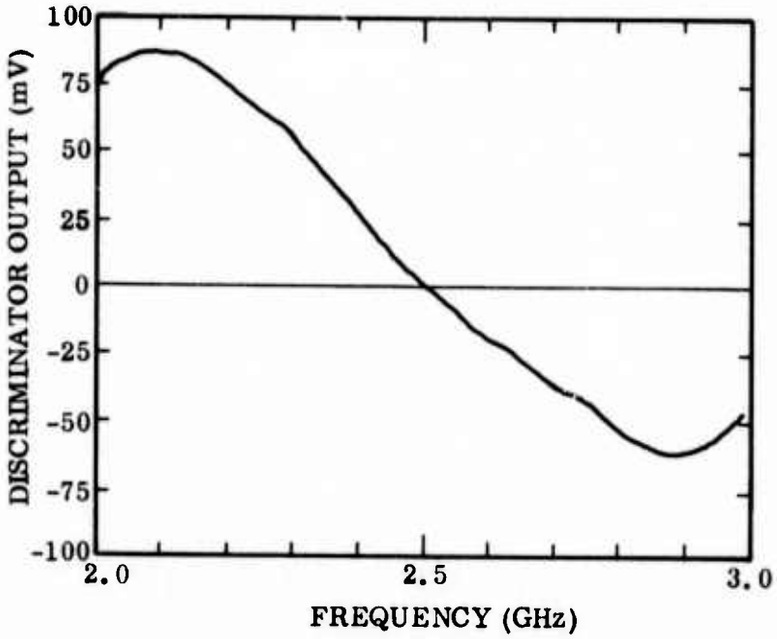

Fig. 3-10 Performance Characteristic of the Final Wideband FM Discriminator

oscillator levelled between 10 MHz to 1 GHz. The upper trace shows the amplified output of the baseband amplifier: clearly the amplification is constant within the band of 10 MHz to 550 MHz. Figure 3-13 shows the recovered baseband signal which is swept between 10 and 450 MHz by the levelled sweeper after FM discrimination and lowpass filtering. It is seen that between 50 MHz and 470 MHz, the output varies by approximately 15 dB. Since this is not most ideal for a communication system, a compensation network was incorporated in the VCO's driver to obtain a better response. As a result, the frequency response is indeed improved as shown in Fig. 3-14. Between 50 and 470 MHz, the relative variation is only about 5 dB. This version was therefore used in the tests.

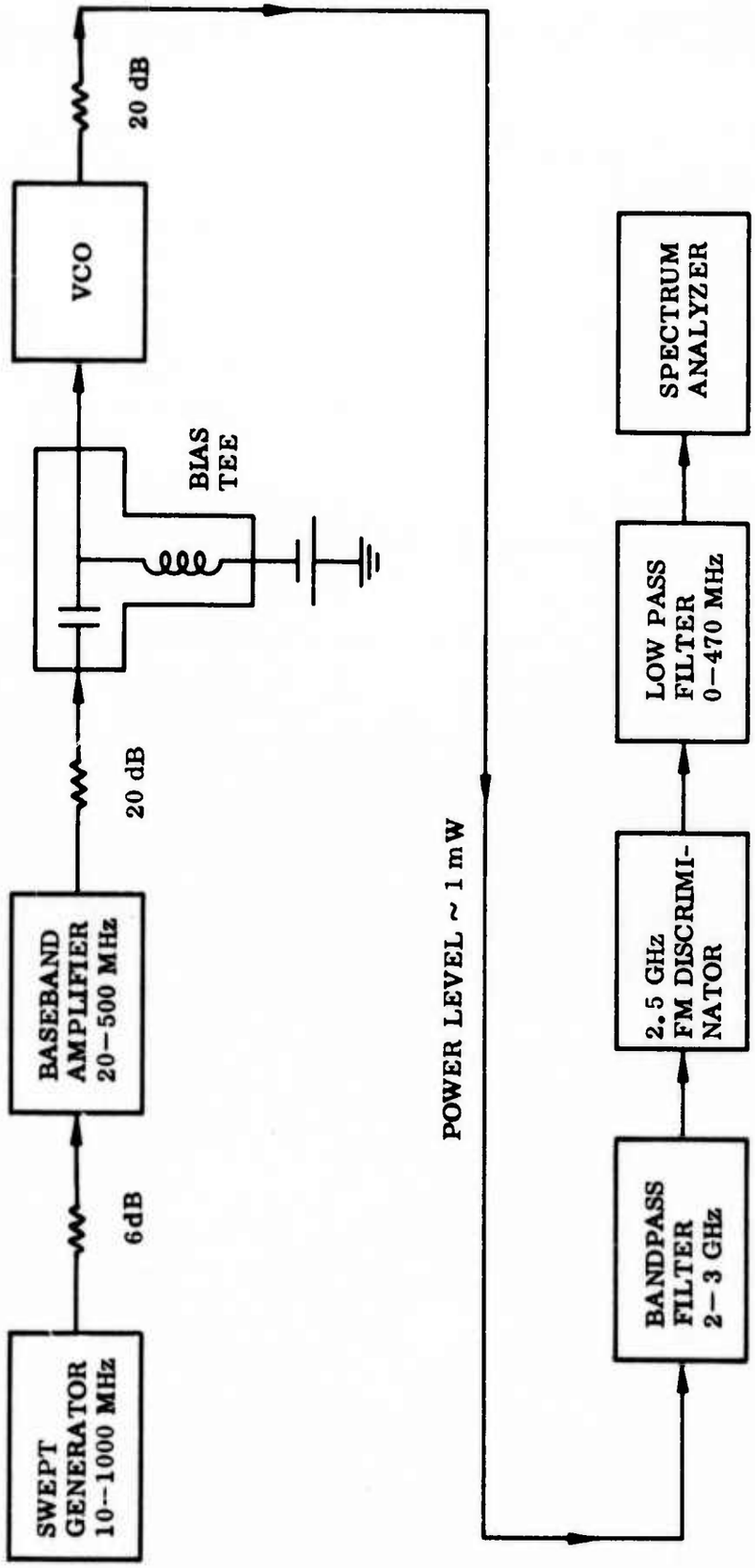

Fig. 3-11 Experimental Setup for the VCO/FM Discriminator Tests

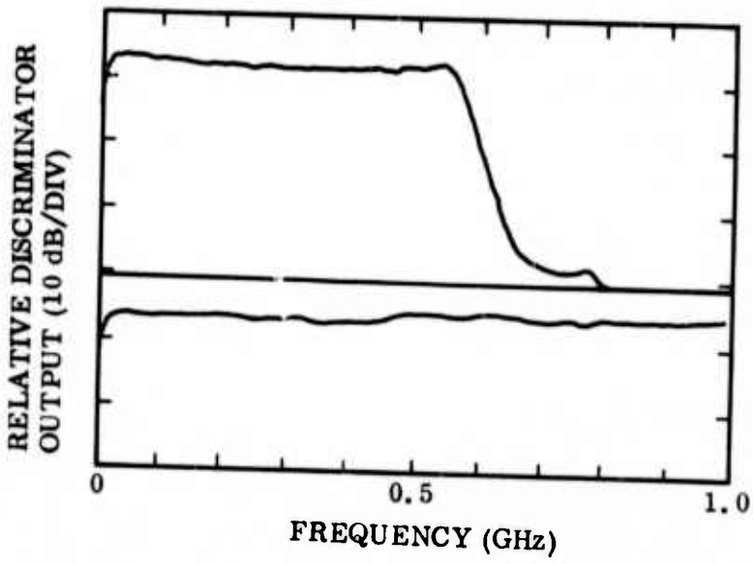

Fig. 3-12 Frequency Response of VCO/FM-Discriminator Test Components. Lower Trace: levelled swept generator output. Upper Trace: VCO Driver amplifier output when swept by the levelled sweeper

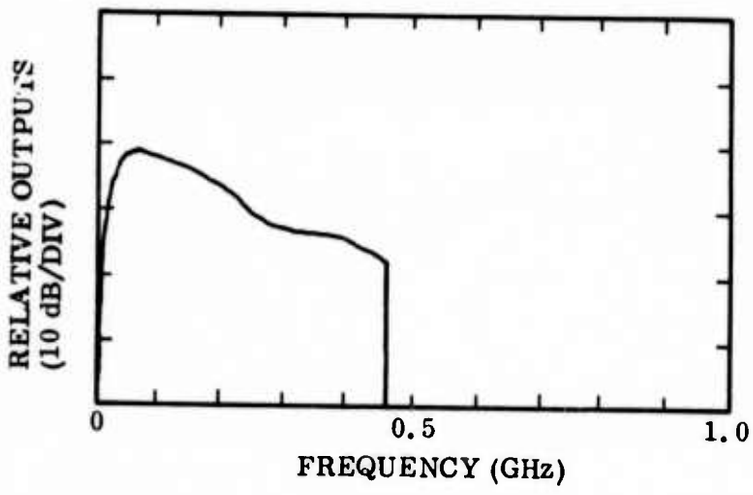

Fig. 3-13 Output of the FM Discriminator When the VCO Is Swept Between 10 and 470 MHz by the Levelled Sweeper and Driver Amplifier

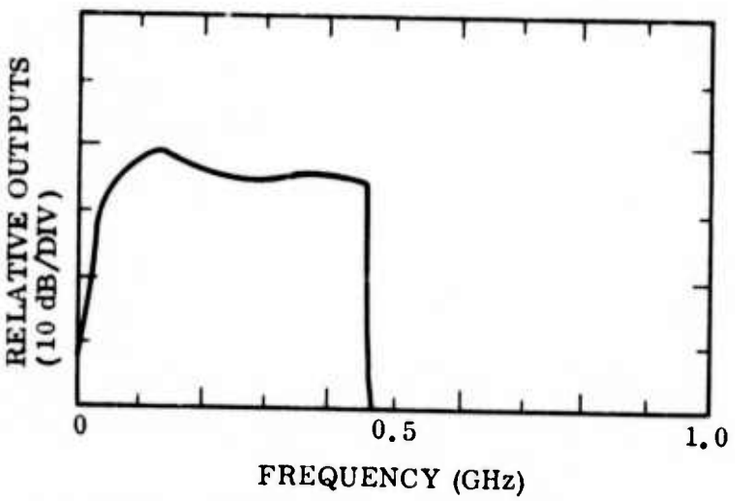

Fig. 3-14 Output of the FM Discriminator When a Compensation Network Is Added to the VCO Driver. Obvious improvement is observed

3.7 SYSTEM IMPLEMENTATION

The system layout is essentially a hardware copy of the block diagrams shown in Figs. 2-2 through 2-5. Judicious choice of amplifiers and attenuators has to be determined to ensure proper signal levels so that signal-to-noise ratios are maximized and cross-talks are minimized.

3.7.1 The 2-Gbit/sec System

Figure 3-15 shows the transmitter end of the laboratory system transmitting 2-Gbit/sec digital data. The components found in the lower and upper shelves are identified below.

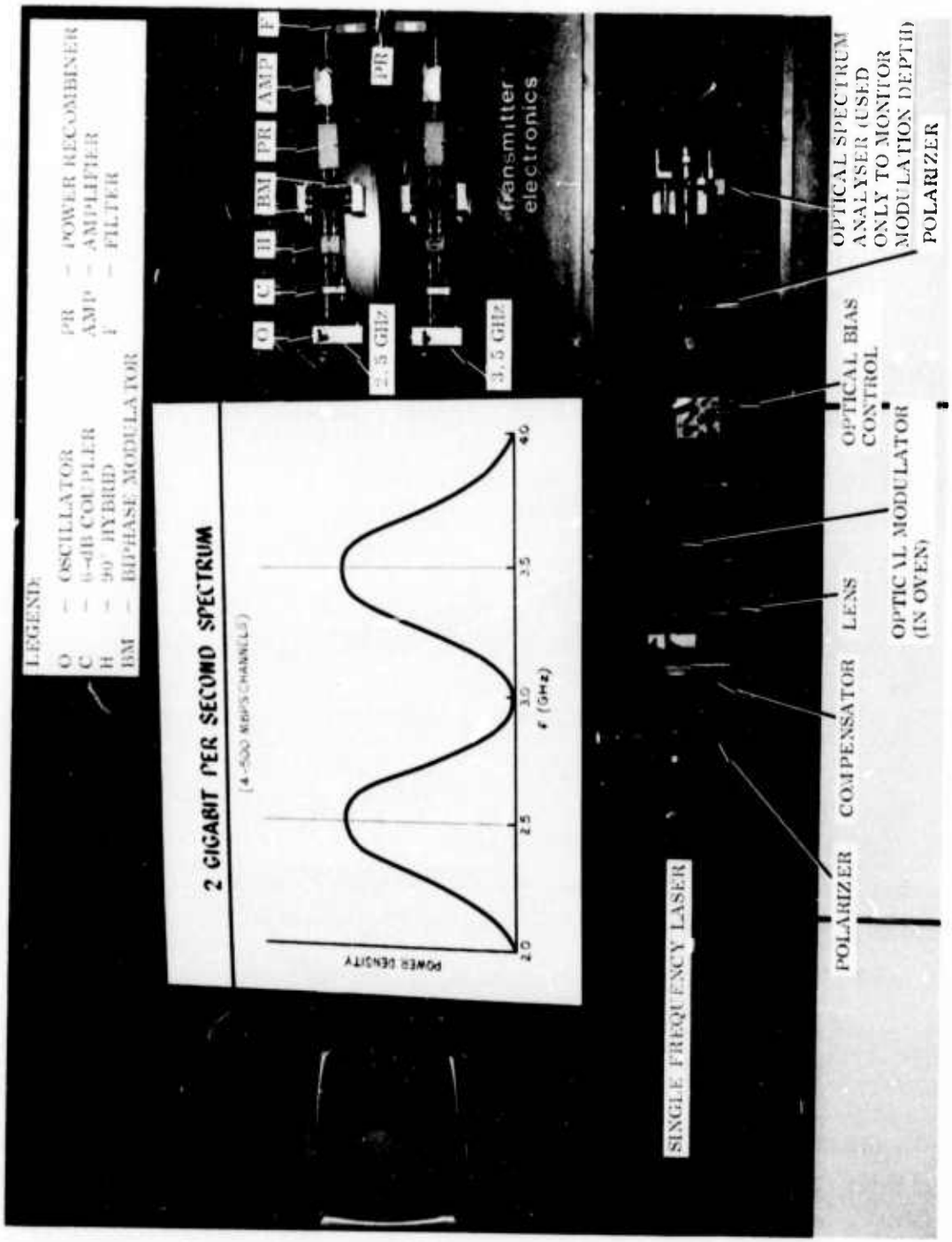

Fig. 3-15 Transmitter of 2-Gbit/sec Laboratory Optical Communication System

On the lower shelf, the optical components in this system are shown. These consist of:

- A single-frequency laser (a commercial ion laser is shown used, to facilitate initial alignments and tests)
- A polarizer, which sets the light polarization at the desired 45-deg angle to the optical compensator and modulator crystal axes
- A servo-motor-driven optical compensator, which automatically sets the optical bias for the modulator
- A focusing lens, which places the optical beam waist at the center of the modulator crystal
- The electrooptical modulator
- An optical bias control unit, which senses the static optical bias condition of the modulator and produces an error signal to drive the compensator to quarter-wave optical-bias
- An output polarizer which converts optical polarization modulation into intensity modulation

An optical spectrum analyzer is shown in Fig. 3-15, but this is used only for monitoring purposes.

On the upper shelf, the transmitter electronics are shown. Components for the two subbands – one derives its subcarrier signal from a 2.5-GHz oscillator and the other from a 3.5-GHz oscillator – are clearly shown. Each subband includes identical types of components consistent with the frequency band. For instance, in the 2- to 3-GHz subband, power from the 2.5-GHz oscillator passes through a 6-dB coupler, with the main output directed to the receiver as the phase reference signal. The -6 dB output passes through a 90-deg hybrid to provide the "in-phase" and the "in-quadrature" channels. Each channel is then biphase-modulated at 500 Mbit/sec by the biphase modulator. The two channels are recombined in the power recombiner, amplified, and filtered to give a QPSK-modulated 2.5-GHz output. This is combined with the QPSK-modulated 3.5-GHz output to give a composite signal containing 2-Gbit/sec total data in a dual QPSK modulation format.

An illustration of the spectrum of the QPSK-modulated 2-Gbit/sec data, using two subcarriers as is done here, is shown in the center of Fig. 3-15. It should again be emphasized here that if PR generators at higher data rates (e.g., 1 Gbit/sec) were readily available, the entire 2-Gbit/sec data transmission could have been achieved using only one subcarrier (e.g., 3 GHz). The reasons for using two subcarriers are:

(1) To make up the desired 2-Gbit/sec data rate in the most convenient way

(2) To show that different data streams can be modulated onto different subcarriers which can then be multiplexed in the transmitter electronics and demultiplexed in the receiver electronics

Figure 3-16 shows the receiver end of the laboratory system. The optical system is again on the lower shelf, consisting simply of an optical attenuator, a focusing lens, and a photodetector (a static cross-field multipler tube – CFPMT – is shown). A different CFPMT from the one purchased under this contract was used in these measurements because this tube did not appear to have the objectionable resonance at 2.5 GHz. From the CFPMT, the detected microwave signal is directed to the receiver electronics, shown in the upper shelf. The signal is divided into two halves in the 3-dB coupler: each half is used for the demodulation of digital data in one subband. Again, the microwave components used for both subbands are identical in type, the only difference being in the frequency response. For instance, for the lower subband, the signal is filtered to give the 2- to 3-GHz components and amplified. This is then again divided into two halves, each half becoming the input signal for a biphase demodulator (BDM). The phase reference signal for a given subband comes from the 6-dB coupler in the transmitter, and is passed through a precision phase-shifter. At the BDM, therefore, the reference signal has a precise phase relationship to the input signal to effect proper demodulation. The reference signal is split by a 90-deg hybrid into an "in-phase" and an "in-quadrature" component; each component is directed to a BDM for the demodulation of a channel. This has been discussed in much detail in the Third Semiannual Technical Report (Ref. 4). As a result, four streams of 500-Mbit/sec data, identical to the outputs from the word generators, are obtained. These are shown displayed on the sampling oscilloscope on the upper shelf.

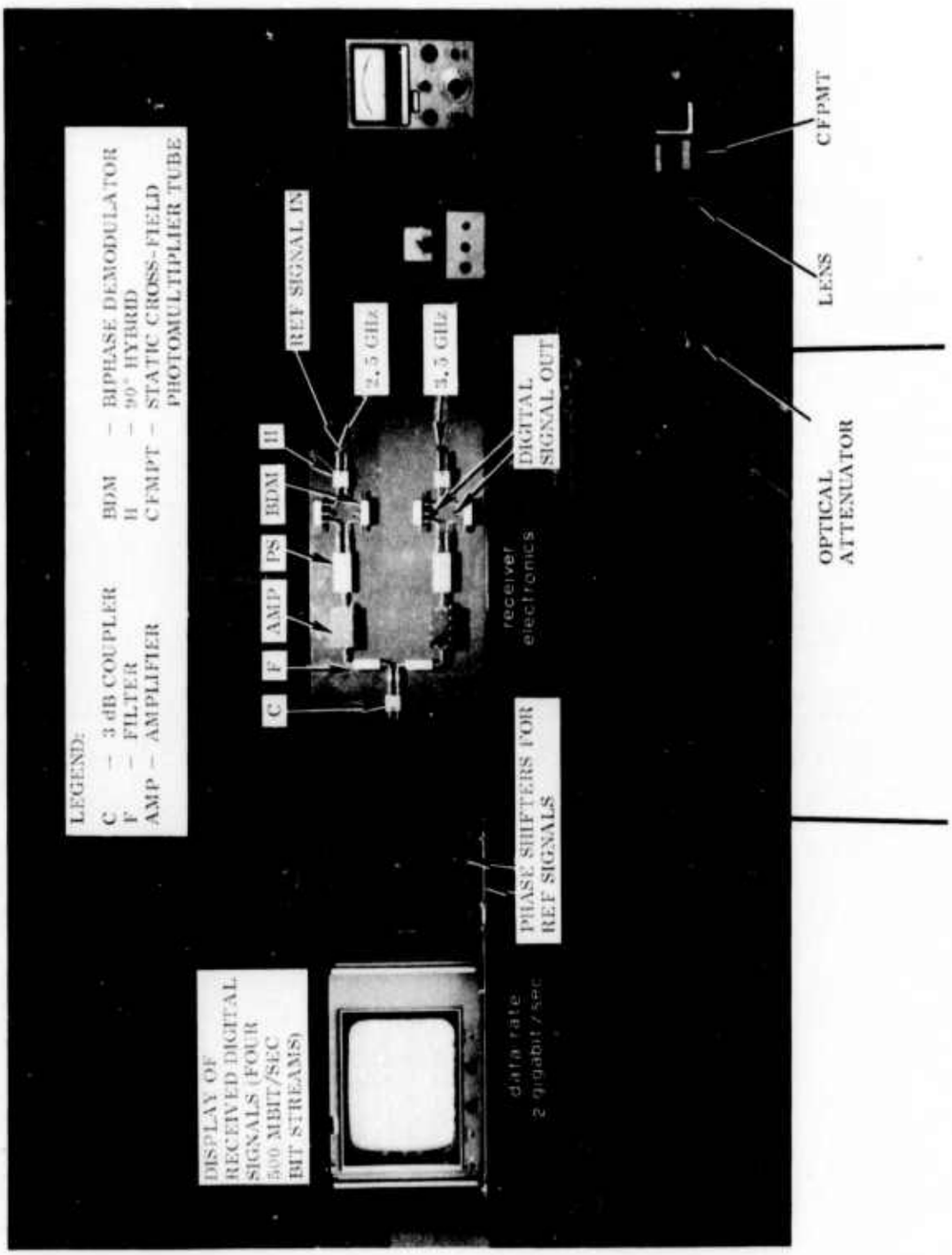

Fig. 3-16 Receiver of 2-Gbit/sec Laboratory Optical Communication System

3.7.2 The 1-GHz FM-Analog and 1-Gbit/sec Digital System

The digital portion of this system is identical to one of the digital channels shown in Figs. 3-15 and 3-16. Specifically, the one that is used in this system has its subcarrier frequency at 3.5 GHz.

The FM-analog portion uses a 2.5-GHz subcarrier, onto which four local TV channels (Channels 4, 5, 7 and 9) and a narrowband FM music at a carrier frequency of 400 MHz are modulated. Figure 3-17 shows a detailed block diagram of the hardware and the monitoring instrumentation used in the transmitter. Various filters, amplifiers, and attenuations are inserted into the system to ascertain minimum intermodulation, to maintain good signal-to-noise ratios, as well as to minimize reflections between components. The implementation here is mainly an experimental one – by trial and error – to determine the causes of, and consequently eliminate or minimize, various undesirable effects. In particular, the VCO bias and drive level have to be adjusted quite stringently to attain good signal-to-noise ratios and minimum intermodulation. This is achieved in the laboratory as indicated by the system test results reported in Section 4.

Figure 3-18 shows a detailed block diagram of the receiver. Again, the implementation is an experimental one. However, sinee the power levels being dealt with in the receiver are rather low (milliwatt and below), saturation or intermodulation is not a problem. The main undesirable effects to minimize are refleetions between components. To this end, isolators and attenuators have been inserted wherever required.

Results on system measurements are presented in Section 4.

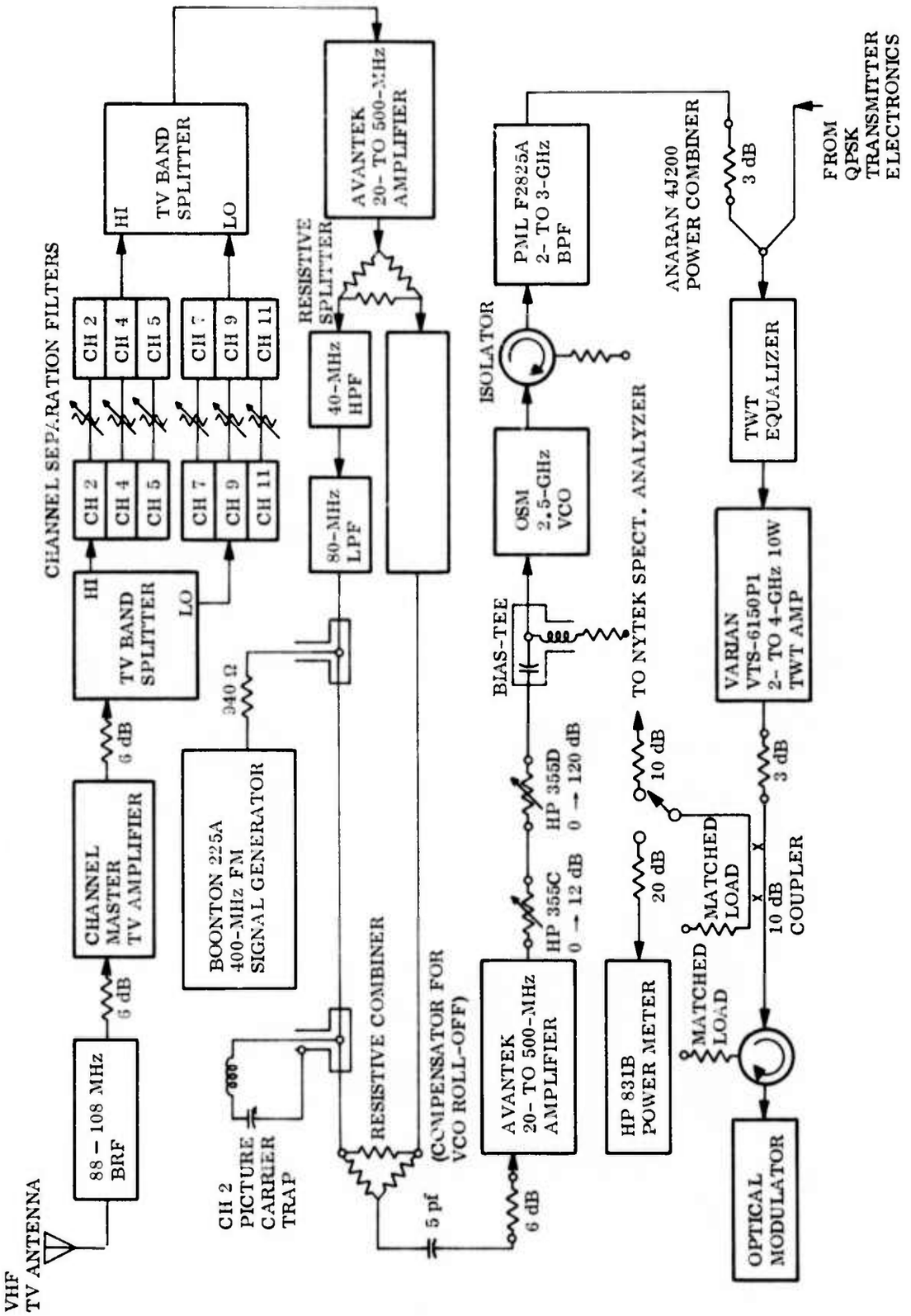

Fig. 3-17 FM Transmitter Electronics. BRF = Band Reject Filter; BPF = Bandpass Filter; LPF = Lowpass Filter; HPF = Highpass Filter

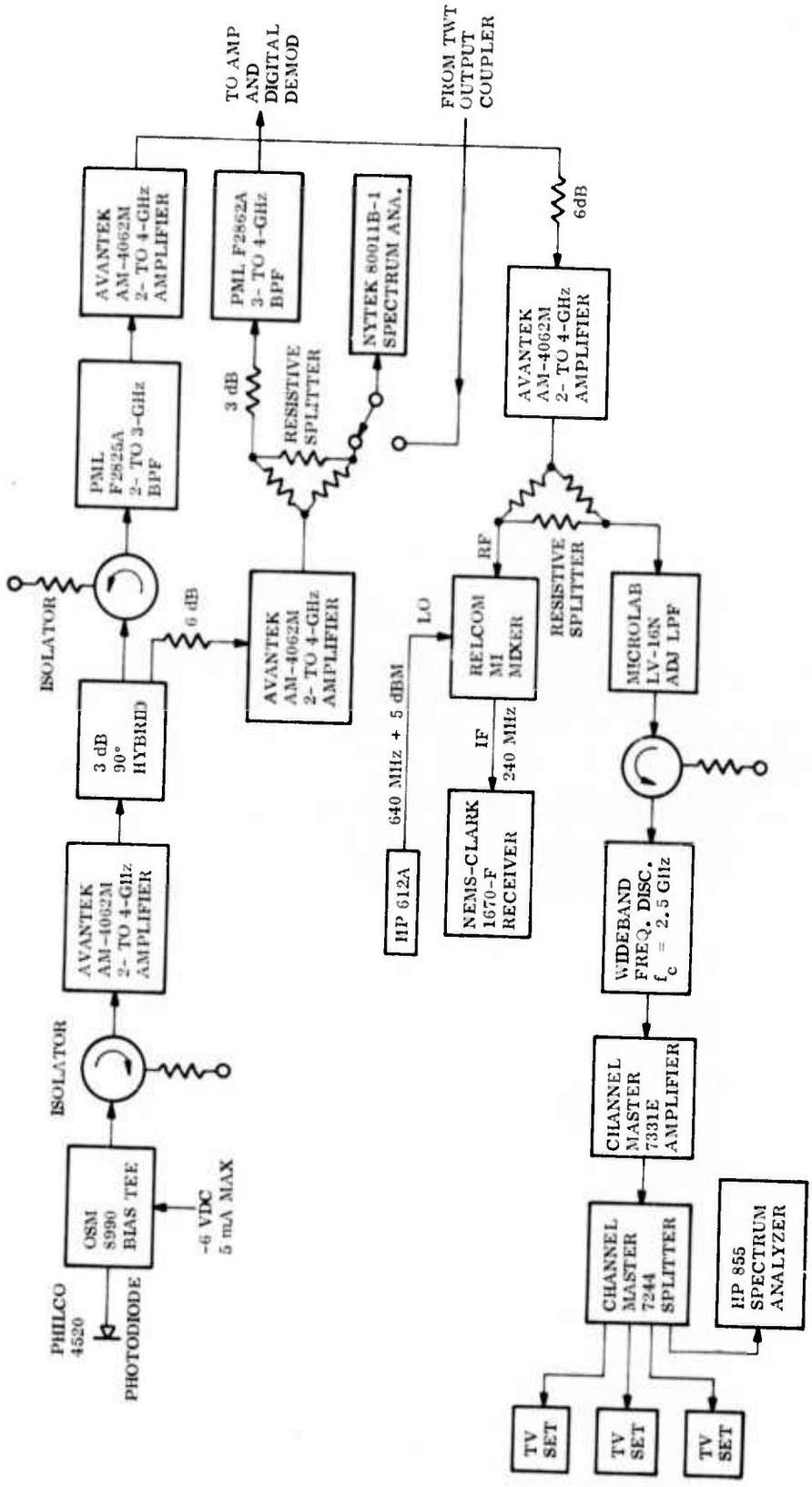

Fig. 3-18 FM Receiver Electronics. BPF = Bandpass Filter; LPF = Lowpass Filter

Section 4
SYSTEM TESTS

Experimental results of critical components such as the optical modulator, the voltage controlled oscillator, etc., as well as those of subsystem tests have been discussed in the earlier sections where appropriate. Only the system test results will be discussed in this section.

4.1 QPSK DIGITAL MODULATION RESULTS

Work on the quadriphase-shift-keying digital modulation was performed during the first half of the year as a preliminary check of the system performance. Results obtained are shown in Figs. 4-1, 4-2, and 4-3. These figures show the typical results of the 2-Gbit/sec laboratory communication demonstration. Figure 4-1 is a sampling scope display of the 2-Gbit/sec data received via the laser link. A total of four 500-Mbit/sec channels are displayed: two of the channels are transmitted through the 2.5-GHz subcarrier, and two are transmitted through the 3.5-GHz subcarrier. All channels show good recovered signals.

Figures 4-2 and 4-3 show the degradation that takes place in the signals after being transmitted through the laser link. This includes the degradation due to the electro-optic modulator and the photodetector. Each figure is for the data over a particular subcarrier: the top two traces show the sampling scope display of the two 500-Mbit/sec data outputs that result from a direct connection (hardwire) from the traveling-wave tube amplifier, with suitable attenuation, to the microwave receiver. The bottom two traces show the two 500-Mbit/sec outputs that result from the transmission over the laser link. These tests were run using a commercial argon ion laser, operating single-mode, single-frequency at $\lambda_o = 0.5145\ \mu m$. The visible wavelength, rather than $1.06\ \mu m$, was used for these initial tests because of the ease of optical alignment and better photodetector response.

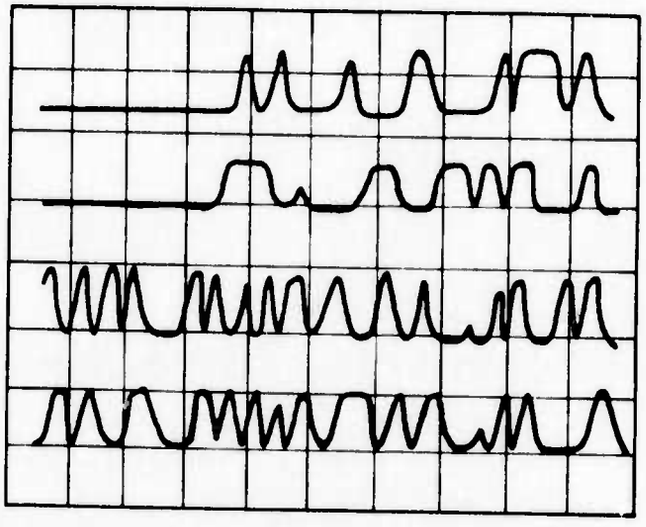

Upper Two Traces: 500 Mbit/sec each on 2.5-GHz subcarrier
Lower Two Traces: 500 Mbit/sec each on 3.5-GHz subcarrier

Fig. 4-1 Sampling Scope Display of Four 500-Mbit/sec Streams Transmitted Through the Laser Link

The traces in Figs. 4-2 and 4-3 show that there is not a one-to-one correspondence between the data bits in the upper traces and those in the lower traces, because the amount of delay in the laser transmission and reception causes a different portion of the PR signal to appear on the oscilloscope, and no provision has been made in these experiments to compensate for this difference in delay. The important aspect of these data is to show the degree to which the character of the data waveform is degraded. From these traces, it is clear that the rise and fall times are lengthened and the corners rounded. However, it is also clear that the bits are still readily recognizable as ones or zeroes even to the eye, although those in Fig. 4-3 appear to be noisier. This noisy performance arises from the fact that the traveling-wave tube used has relatively lower gain at the high-frequency end, and that the cross-field photomultiplier tube (CFPMT), which also has a lower response at the high-frequency end, is used in these measurements. It is estimated that by using matched-filter detection, the data should be recovered with 2- to 3-dB degradation in performance from the theoretical integrate-and-dump performance.

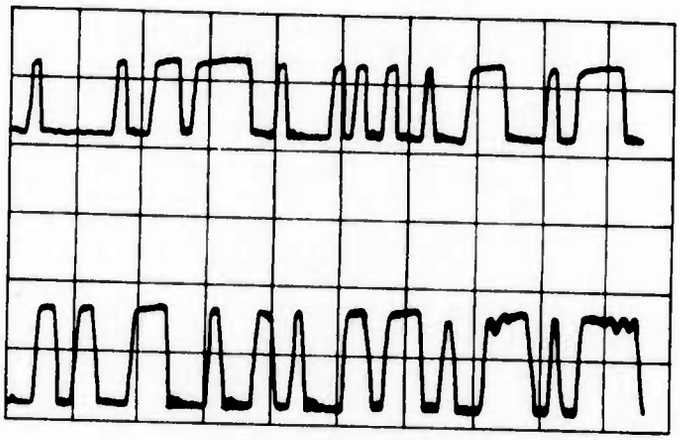

a. Direct connection between transmitter and receiver electronics

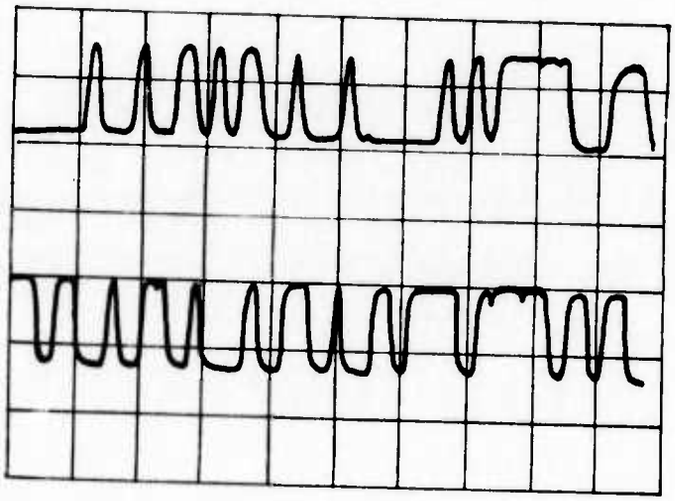

b. As received through the laser link (TWT drive power 4 W: both 2.5-GHz and 3.5-GHz channels on)

Fig. 4-2 Waveforms of Two 500-Mbit/sec Streams on 2.5-GHz Subcarrier Frequency With Simultaneous 1-Gbit/sec Digital Signal on 3.5-GHz Subcarrier

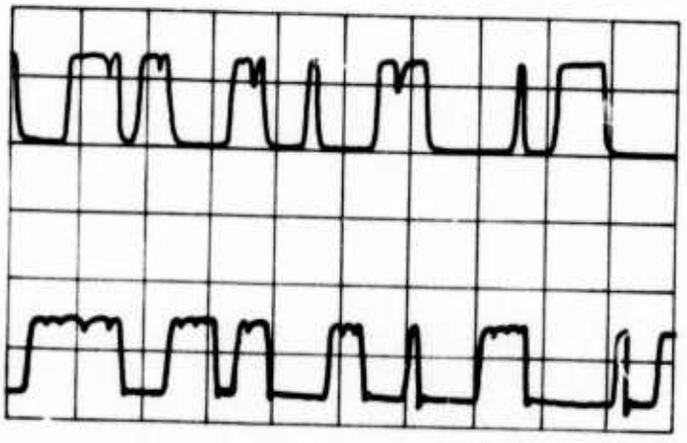

a. Direct connection between transmitter and receiver electronics

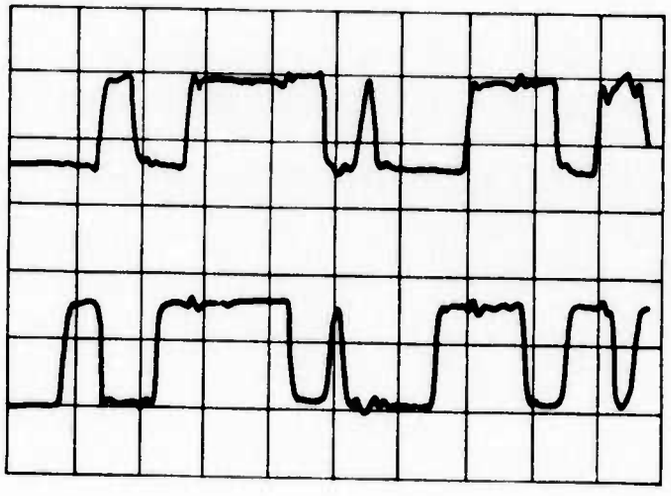

b. As received through the laser link (TWT drive power 4 W: both 2.5-GHz and 3.5-GHz channels on)

Fig. 4-3 Waveforms of Two 500-Mbit/sec Streams on 3.5-GHz Subcarrier Frequency With Simultaneous 1-Gbit/sec Digital Signal on 2.5-GHz Subcarrier

The performance for the 2-Gbit/sec transmission shown above is considered good for this feasibility demonstration since it shows that the system does have the designed bandwidth of 2 GHz and will accept the desired high data rate. Not much fine tuning of the system was done because this demonstration was made purely to ascertain the feasibility of transmitting 2 Gbit/sec data. In any event, the main thrust of this contract is to obtain the 1-GHz/sec analog signal and the 1-Gbit/sec digital signal demonstration to be discussed in subsection 4.2.

4.2 FM ANALOG AND QPSK DIGITAL MODULATION RESULTS

The main thrust of this feasibility study is the transmission of a 1-GHz analog and a 1-Gbit/sec digital data over a 1.06-μm laser beam. Therefore, much "debugging" and refinements have been made for this system. The results obtained unequivocally demonstrate the feasibility of such a transmission in the laboratory.

Initial tests on this transmission were done during the first six months using the visible laser. The 3.5-GHz subcarrier was used for the analog signals, and the 2.5-GHz subcarrier was used for the digital signals. (The use of these subbands was different from that shown in Fig. 2-4, as will become clear in the latter paragraphs of this subsection.) Some difficulty was experienced with the 1-GHz analog subsystem as detailed in the following paragraphs.

The first voltage-controlled oscillator (VCO) used for the FM transmission of the analog signals required rather high driving voltages. To provide these high voltages in a 50-Ω system, high drive power is required. This forces the driver amplifier to operate in saturation, thereby causing intermodulation between the various analog signals (local TV channels 4, 5, 7, and 9). In addition, because of the power limitation of the driver amplifier, the FM deviation was rather low so that the received signal-to-noise ratio (S/N) was high. After much effort had been expended in designing frequency filters (traps) and inserting various attenuators and amplifiers to reduce intermodulation, the results were still considered unsatisfactory.

A second VCO was then ordered. This VCO required much less driving power for its operation so that good linearity with reasonable deviation could be obtained. Results showed that intermodulation had been greatly reduced. However, the S/N ratios for the received signals were still rather poor, typically in the 20-dB range. (For good TV picture reception, a S/N ratio in the range of 40 to 45 dB is required.)

The causes for such a low S/N performance are attributed to:

(1) The frequency deviation is still small (~ 35 MHz at a carrier frequency of 3.5 GHz) so that there is only a small amount of signal content in the FM subsystem.

(2) The allowable optical power on the photocathode is limited (~ 5 μW) and the high-frequency response of the CFPMT is poor, causing further reduction of the signal content with respect to system noise.

Consideration was then given to using the lower subband (2.5-GHz subcarrier) for FM analog transmission and the upper subband (3.5-GHz subcarrier) for digital transmission as shown in Fig. 2-4. This change in direction was based on the following facts:

(1) High power (several watts), wideband (dc to 500 MHz) baseband amplifiers are not commercially available. Thus, to minimize intermodulation, frequency deviation has to be kept small; i.e., the signal content is kept small.

(2) The performance of the CFPMT is poorer than expected in the high-frequency end of the band.

(3) In the lower subband, the traveling-wave tube, the photodetectors all have good response so that higher S/N is obtainable.

(4) For the transmission of digital signals, an S/N ratio of 20 dB gives a good signal display, while for the transmission of analog signals, a minimum S/N of 30 dB is required.

In the final demonstration, therefore, the 2.5-GHz subcarrier is used for the transmission of analog signals; onto the subcarrier are modulated local TV channels 4, 5,

7, and 9, as well as a narrowband FM musie (FM about a 400-MHz earrier frequeney). The digital data are modulated onto the 3.5-GHz subearrier by using a QPSK format. At 1-Gbit/sec, the sidebands of the QPSK digital modulation oecupy the entire 3- to 4-GHz subband. The analog signals used occupy most of the 2- to 3-GHz subband. Figure 4-4 shows the complex microwave frequeney spectrum of this modulation format as it is deteeted at the output of the traveling-wave-tube (TWT) amplifier. (Since the TWT is the driver amplifier for the optieal modulator, this speetrum represents the input signal to the optical modulator.)

In Fig. 4-4, the lower subband, viz., the 2- to 3-GHz subband, is shown in the left half. A subearrier frequency of 2.5 GHz is shown in the eenter. The upper and lower sidebands of that subearrier are shown on either side. The peaks of the sidebands are loeal TV ehannels 4 and 5, and 7 and 9, as well as the 400-MHz narrowband FM earrier. The two adjacent TV ehannels are barely resolved in this pieture. The upper subband, the 3- to 4-GHz subband, is QPSK-modulated by 1-Gbit/see stream data. It is seen that the frequeney speetrum is quite complex.

After transmission through the optieal beam, the deteeted microwave spectrum is as shown in Fig. 4-5. In this figure, gain of the speetrum analyzer has been adjusted so that the 2.5-GHz subearrier power gives the same amount of deflection as that shown in Fig. 4-4. By eomparing these two figures, it is apparent that the analog signals suffer relatively minor amount of attenuation upon going through the laser beam, while digital signals do suffer a much higher relative attenuation. This higher amount of attenuation in the 3- to 4-GHz subband is primarily due to the lower response of the photodeteetor and the lower optieal modulation index in that subband.

For the analog FM subsystem, it is neeessary to obtain a signal-to-noise ratio of greater than 30 dB before an aceeptable TV pieture ean be obtained. If the signal-to-noise ratio is less than 30 dB, the TV pietures beeome "snowy" and begin to lose details. A good pieture as obtained from a well-directed antenna normally contains a signal-to-noise ratio of 40 to 45 dB. In this demonstration, therefore, most of the

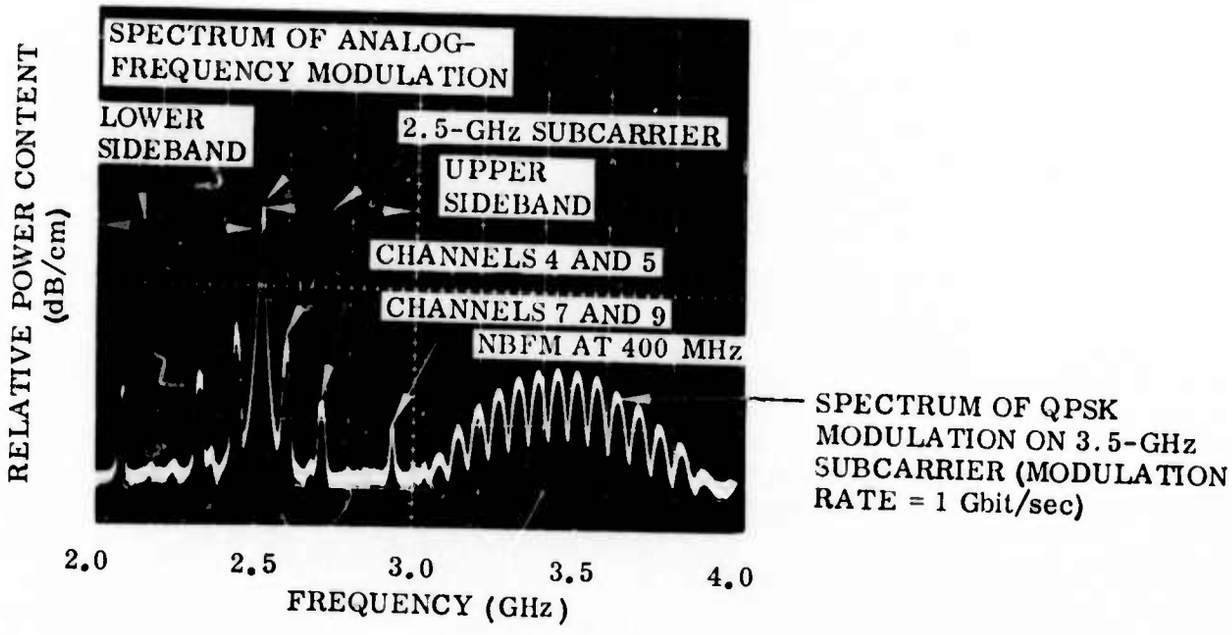

Fig. 4-4 Complex Microwave Spectrum as Seen at the Output of the Traveling-Wave Amplifier. 2- to 3-GHz Subband: Analog Modulation; both upper and lower sidebands are shown. 3- to 4-GHz subband, spectrum of QPSK modulation at 1 Gbit/sec

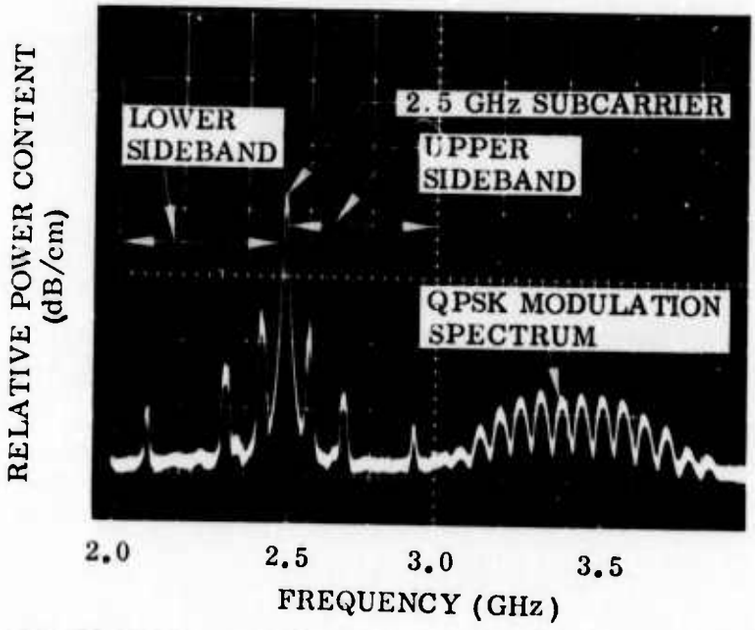

Fig. 4-5 Complex Microwave Spectrum As Seen at the Receiver (After Optical Detection and Microwave Amplification). The spectrum is identical to that shown in Fig. 4-4, except for higher attenuation in the 3- to 4-GHz subband

effort was spent in achieving a signal-to-noise ratio of 30 dB and above. The problems involved in this respect are:

- Signal strength
- Detector sensitivity
- Allowable amplifier gain at various stages
- Proper attenuation or padding between components to avoid multiple reflections and overdrives causing intermodulation

After much effort, signal-to-noise ratios of about 30 dB for all the local TV channels were obtained as shown in Figs. 4-6 and 4-7.

Figure 4-6 shows the signals for channels 4 and 5 after transmission through the laser beam, processed, and arriving at the TV monitor sets. It is seen that a signal-to-noise ratio for the picture carrier of approximately 35 dB is obtained for both channels 4 and 5. Figure 4-7 shows the received signals for channels 7 and 9 – approximately 35 dB of signal-to-noise is obtained for both channels. In contrast, the TV signals as obtained directly from TV antennas and through TV amplifiers are shown in Figs. 4-8 and 4-9: Fig. 4-8 is the one for channels 4 and 5, and Fig. 4-9 is the one for channels 7 and 9. In Fig. 4-8, FM broadcasting stations were also seen. These were filtered out at a later stage. It is seen that typically, signal-to-noise ratios of about 45 dB were obtained for all these channels (picture carrier to noise). Thus, by going through the system, a degradation of 10 dB in signal-to-noise ratio is typically obtained. This degradation is considered reasonable for this feasibility demonstration since all the electronics and electrooptic components can still be greatly improved for this purpose.

For the 1-Gbit/sec digital data transmission, typical results of the data bits as they pass through various stages of the system are as shown in Fig. 4-10. A total of 7 oscillographs are shown, each oscillograph containing two traces. Throughout this series, the horizontal positions of both traces have been adjusted so that the upper traces show throughout the same portion of a 500-Mbit/sec stream and so that the lower traces show throughout the same portion of the other 500-Mbit/sec stream.

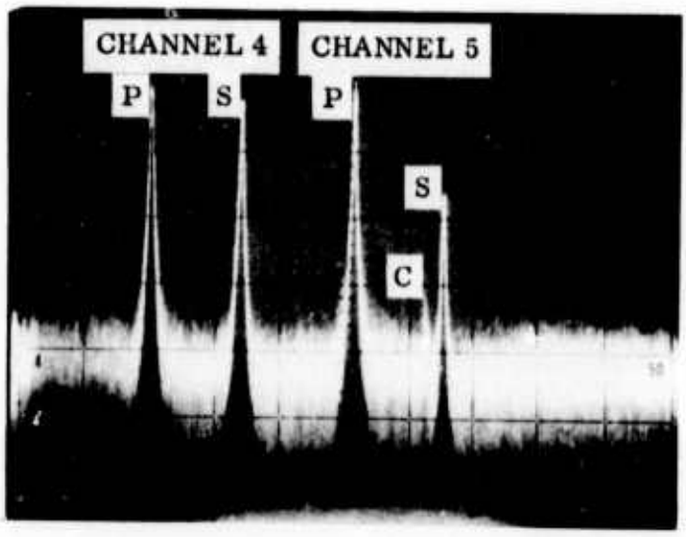

Fig. 4-6 Spectrum of TV Channels 4 and 5 After Transmission Through 1.06-μm Beam, Detection by a Germanium PIN Diode, and Processed to be Ready for Display on TV Sets. P = Picture Carrier; S = Sound Carrier; and C = Chromatic Subcarrier

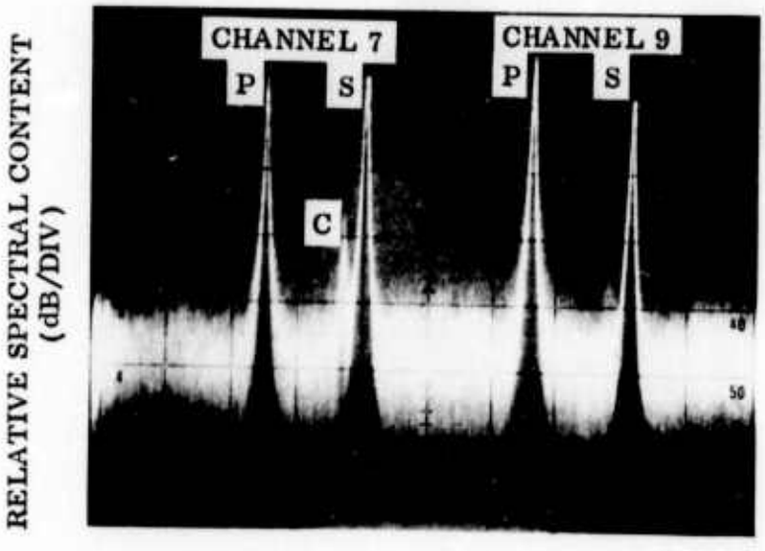

Fig. 4-7 Spectrum of TV Channels 7 and 9 After Transmission Through 1.06-μm Beam, Detection by a Germanium PIN Diode, and Processed to be Ready for Display on TV Sets. P = Picture Carrier; S = Sound Carrier; and C = Chromatic Subcarrier

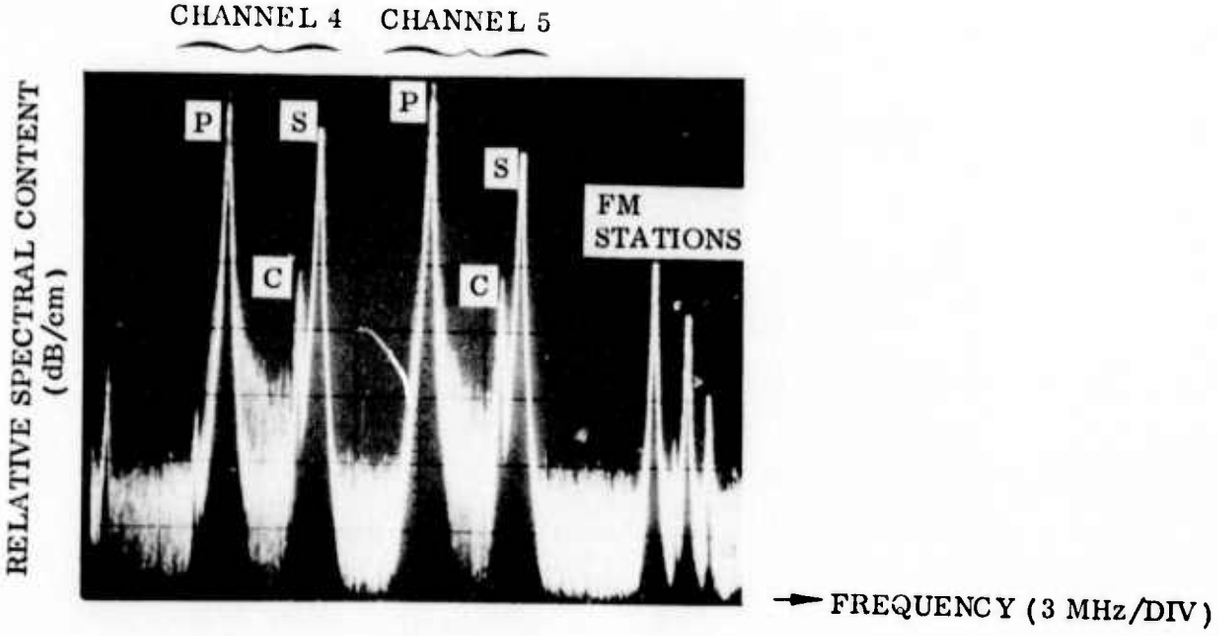

Fig. 4-8 Spectrum of TV Channels 4 and 5 As Received From a High-Gain Antenna and Amplified. FM Broadcasting Stations are also received; these are filtered out later in the system. P = Picture Carrier; S = Sound Carrier; and C = Chromatic Subcarrier

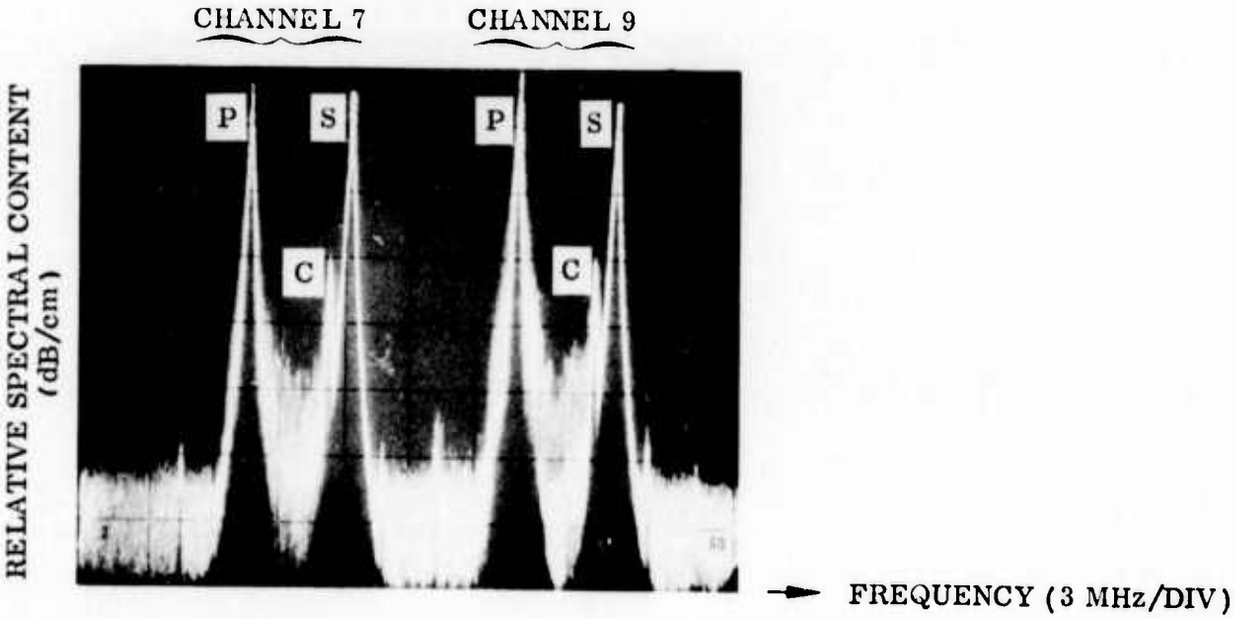

Fig. 4-9 Spectrum of TV Channels 7 and 9 As Received From a High-Gain Antenna and Amplified. P = Picture Carrier; S = Sound Carrier; and C = Chromatic Subcarrier

a. Outputs From the PR Word Generator

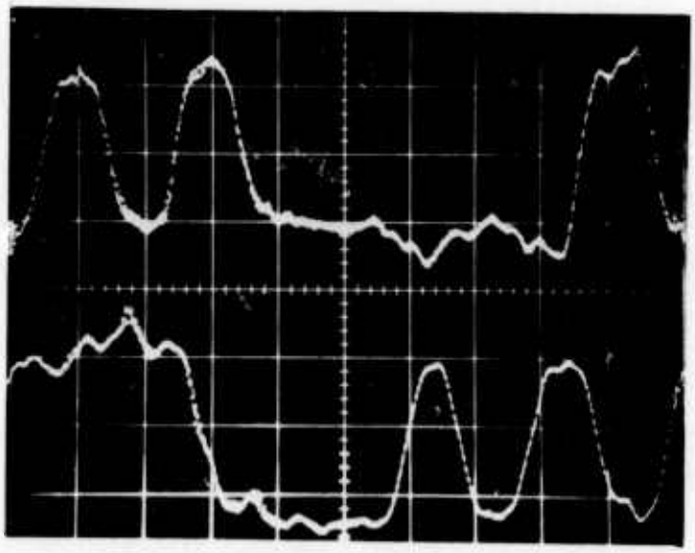

b. After Modulation Onto the QPSK Modulator and Subsequently Demodulated by the QPSK Demodulator and Amplified. Direct cable connection between the Modulator and the Demodulator (40 ft of RG 142/U). Slight ringing was observed

Fig. 4-10 Waveforms of the Two 500-Mbit/sec Data as They Appear at Various Stages in the Laboratory Communication System. Each trace in an oscillograph is a portion of a 500-Mbit/sec stream, biphase modulated onto the 3.5-GHz subcarrier. Vertical scale: linear; horizontal scale = 2 nsec/cm

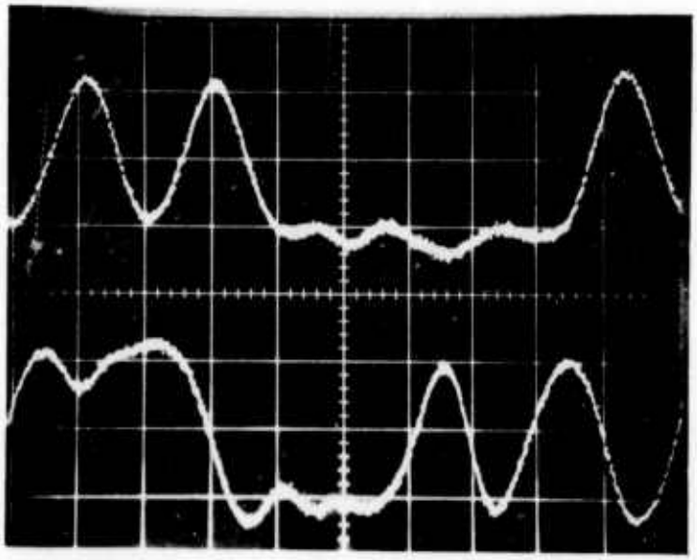

c. Same as in Fig. 4-10b Except for the Addition a 3- to 4-GHz Bandpass Filter at the Transmitter Output, and Another 3- to 4-GHz Filter at the Receiver Output. Much rounding-off of the corners was observed.

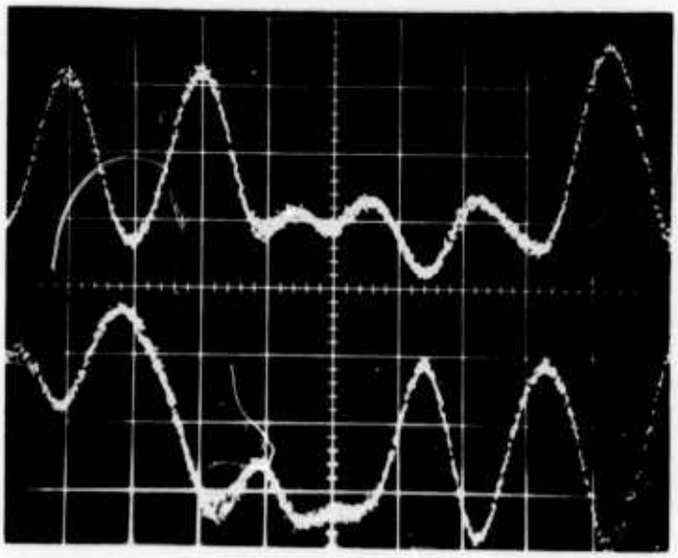

d. Same as in Fig. 4-10c Above, Except for the Addition of the TWT. Much ringing due to phase-distortion in the TWT was observed.

Fig. 4-10 (Cont.)

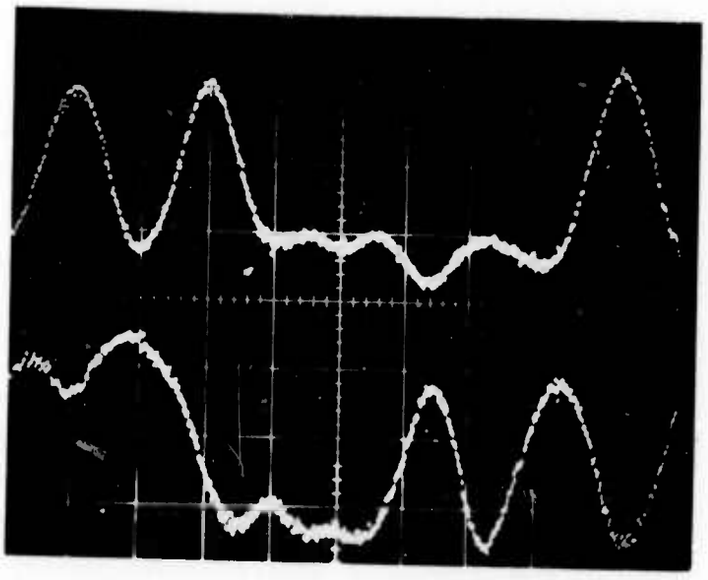

e. Same as Fig. 4-10d, Except for the Addition of a Phase Compensation Network at the Input of the TWT to Minimize Ringing

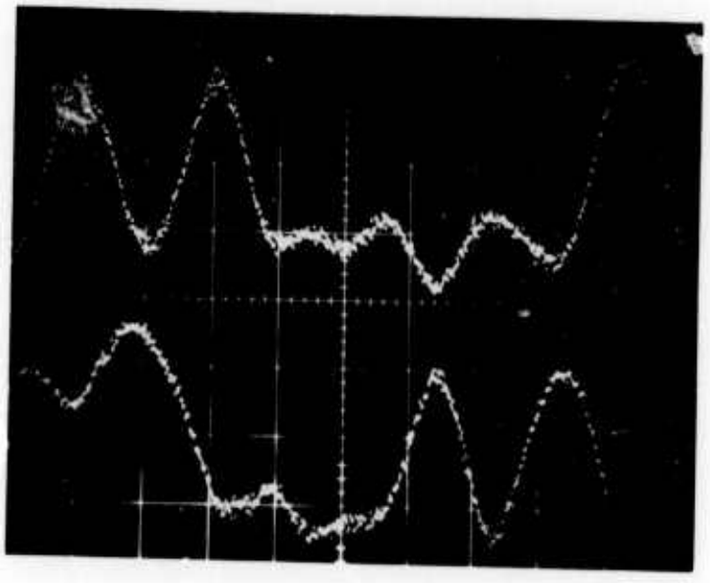

f. Same as Fig. 4-10e Above, But With the Data Transmitted Over the 1.06-μm Laser Beam Instead of Direct Cable Connection. Additional ringing due to phase distortions in the optical modulator and photodetector was observed

Fig. 4-10 (Cont.)

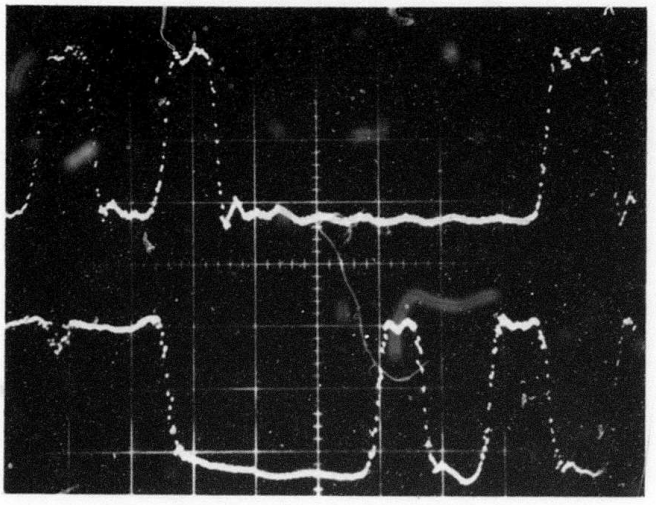

g. Same as Fig. 4-10f Above, But With the Addition of a Clipping Amplifier. The waveform is nearly completely restored.

Fig. 4-10 (Cont.)

That is, adjustments in relative time delay were made for every oscillograph so that the same portions of the 500-Mbit/sec streams are displayed on the sampling scope to afford easy comparison.

Figure 4-10a shows the outputs from the PR word generator: good, clean waveforms are obtained. Figure 4-10b shows the 500-Mbit/sec streams after demodulation from the 3.5-GHz subcarrier using direct cable connection between a QPSK modulator and demodulator. The connection is made with a 40-ft length RG-142/U cable. Distortions due to modulators, demodulators, and amplifiers, etc., in the QPSK system are observed. Thus, Fig. 4-10b is the direct wire (hardwire) results of the electronics of the system, and shows the distortions imposed by the low-level electronics. Figure 4-10c shows again a display of the data bits, hardwired the same way as Fig. 4-10b above, except for the addition of 3- to 4-GHz bandpass filters for each data stream:

one at the transmitter low-level amplifier output, and another at the receiver amplifier output. Much rounding-off of the data bits is observed. Figure 4-10d shows the same data streams after the driving amplifier for the optical modulator (the TWT) operating at a 3-W drive level has been added. Additional distortions, primarily phase distortions causing ripples in the data streams, have now been added and are observed. As a result of this phase distortion, a phase compensator was added at the output of the traveling-wave tube. The result of using that phase compensator is shown in Fig. 4-10e: the distortion has been considerably reduced.

Figure 4-10f shows the detected signal after the data streams have been transmitted over the 1.06-μm laser link, all the electronics being the same as that for Fig. 4-10e. Comparison between these two figures shows that additional phase distortion has occurred in Fig. 4-10f. These distortions occur in the electrooptical modulator and the photodetector since these two are the only added elements in Fig. 4-10f. However, by passing these waveforms through a clipping amplifier, much waveform restoration is obtained as shown in Fig. 4-10g. Comparing Fig. 4-10g with 4-10a (that from the generator output) shows that there is only a small amount of distortion through the entire process. Again, by using matched filter detection techniques, it is estimated that the results obtained in this feasibility demonstration should not be worse than 2 dB from the theoretical integrate-and-dump performance.

Section 5
LABORATORY DEMONSTRATIONS

The 2-Gbit/sec laboratory optical communication system was demonstrated in August 1973 to Dr. R. E. Behringer, ONR Pasadena Office, and Dr. F. Quelle, ONR Boston Office. The 1-GHz analog FM and 1-Gbit/sec digital QPSK laboratory system was demonstrated in April 1974 to Dr. R. E. Behringer, ONR Pasadena Office.

A full-scale demonstration and discussion were given in June 1974 to the following government personnel:

R. E. Behringer	ONR/Pasadena
F. Quelle	ONR/Boston
M. White	ONR/Boston
J. Ivory	ONR/Chicago
J. Soules	ONR/Cleveland - Pasadena
I. Rowe	ONR/New York
A. Wood	ONR/Boston

Section 6
CONCLUSIONS AND RECOMMENDATIONS

The results of this year's work clearly shows that all the program objectives have been met and exceeded: Optical communications in the laboratory having a bandwidth of 2 GHz are feasible using a 1.06-μm laser beam. In particular, two laboratory systems have been demonstrated: one is a 2-Gbit/sec digital data-transmission system employing QPSK modulation on microwave subcarriers; the other is the simultaneous transmission of a 1-GHz analog-FM signal and a QPSK modulation using a 1-Gbit/sec digital data stream.

For the 2-Gbit/sec digital data transmission, good digital waveforms are recoverable; it is estimated that the performance of the system is perhaps no worse than a degradation of 2 dB from the theoretical integrate-and-dump operations. For the simultaneous transmission of analog and digital data, typical results show that a signal-to-noise ratio of greater than 30 dB can be obtained for the analog signals (local TV channels). This performance corresponds to a degradation of about 10 dB, due to the transmission over the optical link and required electronics, from those signals received directly from a high-gain TV antenna (the starting signal). The digital part shows the same recoverable results as in the 2-Gbit/sec data transmission case.

Since the feasibility of such communications has been demonstrated in the laboratory, the next step will be to improve the component performance, both electrooptic and electronic, so that phase and amplitude distortions can be minimized in the system. Another pressing development is that of a wideband photodetector with flat frequency response up to 4 GHz, high sensitivity, low noise, reasonable current-saturation limit, and long lifetime.

Section 7
REFERENCES

1. R. C. Ohlmann, W. Culshaw, K. K. Chow, H. V. Hance, W. B. Leonard, and J. Kannelaud, High-Efficiency, Single-Frequency Laser and Modulator Study, First Annual Technical Report, 30 Sep 1971, Contract No. N00014-71-C-0049, Office of Naval Research/Advanced Research Project Agency

2. -----, High-Efficiency, Single-Frequency Laser and Modulator Study, Second Annual Technical Report, 31 Dec 1972, Contract No. N00014-71-C-0049, Office of Naval Research/Advanced Research Project Agency

3. R. B. Ward and D. G. Peterson, Design Performance Verification I, Technical Report AFAL-TR-73-371, Nov 1973, Air Force Avionics Laboratory, Wright-Patterson Air Force Base, Ohio

4. R. C. Ohlmann, K. K. Chow, J. J. Younger, W. B. Leonard, D. G. Peterson, and J. Kannelaud, High-Efficiency, Single-Frequency Laser and Modulator Study, Third Semiannual Technical Report, 30 Sep 1971, Contract No. N00014-71-C-0049, Office of Naval Research/Advanced Research Project Agency

5. W. R. Kincheloe and M. W. Wilkens, "Phase and Instantaneous Frequency Discriminators," U.S. Patent 3,395,346, Jul 30, 1968

6. M. W. Wilkens and W. R. Kincheloe, Microwave Realization of Broadband Phase and Frequency Discriminators, Stanford Electronics Laboratory, Tech. Rep., 1962/1966-2, Nov 1968, DDC ASTIA Doc. AD 849,757